Reactive compatibilization of poly(styrene-ran-acrylonitrile) (SAN) / poly(ethylene) blends using thiol and epoxy functional SAN

Bayron Garcia Chaparro

Department of Chemical Engineering
McGill University
Montréal, Québec, Canada

2013

A thesis submitted to McGill University in partial fulfillment
of the requirements of the degree of Master of Engineering

Abstract

Well-defined styrene/acrylonitrile (SAN) statistical copolymers with thiol functionality were synthesized for use as a barrier material when melt-blended with epoxy grafted poly(ethylene) (E-PE). SAN was synthesized via reversible addition fragmentation chain transfer polymerization (RAFT) in dimethylformamide (DMF) solution, using dibenzyl trithiocarbonate (DBTC) as chain transfer agent (CTA) and 2, 2'-azobis(isobutyronitrile) (AIBN) as initiator. Typically, SAN copolymers exhibited relatively narrow molecular weight distribution with number average molecular weights ($\overline{M}_n$) of 31.4-37.6 kg·mol^{-1} ($\overline{M}_w/\overline{M}_n$ (PDI) = 1.3-1.4) and a sufficiently high acrylonitrile (AN) incorporation for barrier properties (35-40 mol.%). The trithiocarbonate-containing SAN was reacted post-polymerization via an aminolysis reaction to yield thiol end-functional SAN (SH-SAN). SH-SAN was melt-blended with both E-PE and non-functional poly(ethylene) (PE) in a miniature twin screw extruder at 20 wt.% loading at 180ºC. The SAN dispersed phase morphology of the blend was characterized using scanning electron microscopy and consisted of droplets with volume to surface average diameter ($\langle D \rangle_{sv}$) of 1.3 μm for the reactive E-PE/SH-SAN (80/20 wt.%) blend and 3.8 μm for the non-reactive PE/SH-SAN. For the reactive blend, the dispersed SAN droplets coarsened to $\langle D \rangle_{sv}$ = 2.5 μm, however the droplets remained smaller than the droplets from the SH-SAN/PE blend ($\langle D \rangle_{sv}$ = 3.9 μm). The dispersed SAN domains were reoriented using a channel die to impart elongated domains which would be desirable for barrier materials.

Epoxy grafted SAN (E-SAN) was also synthesized by the terpolymerization of AN, styrene (ST), and glycidyl methacrylate (GMA) via RAFT in DMF solution, using DBTC as CTA and AIBN as initiator. Three E-SAN terpolymers were synthesized at GMA loadings of 5, 10 and 20 mol.% with $\bar{M}_n$s ranging from 34.8-38.3 kg·mol^{-1}, PDI =1.4-1.5 and final AN compositions from 29-40 mol.%.

Résumé

Des copolymères de styrène-acrylonitrile (SAN) bien définis avec des fonctionnalités de thiol ont été synthétisés pour être utilisés comme matériau format une barrière lorsque mélangé au dessus de leur point fusion avec du poly(éthylène) greffé d'époxy (E-PE). Le SAN a été synthétisé via une polymérisation radicalaire contrôlée par transfert de chaîne réversible par addition-fragmentation (RAFT) dans une solution de diméthylformamide (DMF), en utilisant du dibenzyle trithiocarbonate (DBTC) comme agent de transfert de chaîne (CTA) et 2,2'-azo-bis(isobutyronitrile (AIBN) comme initiateur. Typiquement, les copolymères de type SAN présentent une distribution de masse moléculaire relativement étroite avec une moyenne en nombre de ($\bar{M}_n$) de 31.4-37.6 kg·mol^{-1} ($\bar{M}_w/\bar{M}_n$ (PDI) = 1.3-1.4) et suffisamment élevé acrylonitrile (AN) constitution pour les applications de barrières (35-40 %.mol). Une réaction aminolyse induite post-polymérisation SAN avec trithiocarbonate a résulté en SAN avec des groupes thiol fonctionnels aux extrémités (SH-SAN). SH-SAN a été mélangé au dessus de son point de fusion avec à la fois E-PE et du poly(éthylène) (PE) non fonctionnel dans une extrudeuse miniature à double vis (20% m/m à 180ºC). La morphologie de phase dispersée (SAN) du mélange a été caractérisé en utilisant un microscope électronique à balayage, donnant des gouttelettes avec un diamètre moyen (ratio volume à surface) ($\langle D \rangle_{sv}$) de 1.3 um pour le mélange réactif E-PE/SH-SAN (80/20% m/m) et 3.8 um pour non réactif PE/SH-SAN. Pour le mélange réactif, le diamètre des gouttelettes de SAN dispersées a augmenté à $\langle D \rangle_{sv}$ = 2.5um, en demeurant toutefois inférieur à celui

des gouttelettes du mélange SH-SAN/PE ($\langle D \rangle_{sv}$ = 3.9 μm). Les gouttelettes de SAN ont été réorientées en utilisant une matrice de manière à leur donner une forme allongée, désirable pour des matériaux de barrière.

Le SAN greffé d'époxy (E-SAN) a été synthétisé par terpolymérisation de AN, styrène (ST) et méthacrylate de glycidyle (GMA) via RAFT dans une solution de DMF, en utilisant DBTC comme CTA et AIBN comme initiateur. Trois terpolymères de E-SAN étaient synthétisé à GMA compositions de 5,10 en 20 mol.% avec $\bar{M}_n$s allant de 34.8-38.3 kg·mol^{-1}, PDI = 1.4-1.5 et une composition finale de AN de 29-40 %.mol.

Acknowledgements

I would like to thank my supervisor Prof. Milan Marić for his guidance and supervision throughout my project. Thanks also to my research group members; especially Keith and Chi who helped me throughout the process.

I would like to thank the McGill Department of Chemical Engineering for providing the appropriate space and environment. Special thanks go to Sergio Mira, Frank Caporuscio and Emily Musgrave.

I would like to thank the Department of Chemistry for the use of the analytical equipment; special thanks to Frederick Morin for NMR training and Petr Fiurasek in the Centre for Self Assembled Chemical Structures for his assistance with the FTIR, UV-vis, TGA and DSC.

I would like to thank the Natural Sciences and Engineering Research Council of Canada (Collaborative Research and Development Grant) and Imperial Oil Limited (University Research Award) for funding the research.

Table of Contents

1 General Introduction

1.1 Background

Polymer Blends

Polymer blending is an excellent technique for the development of new materials, where the properties of different polymers are combined into the blends. This route is often much less expensive than designing an entirely new polymer to achieve the desired properties.[1] Further, another reason for employing multicomponent blends is the addition of a relatively cheap second component that may reduce the cost of an expensive polymer while maintaining its performance.[2] Polymer blends are classified as heterogeneous (immiscible) or homogeneous (miscible). In heterogeneous blends, many properties of the individual components are retained, particularly those related to phase separation. For example, an immiscible blend of two polymers would exhibit the glass transition temperatures of the individual components. In contrast, miscible blends are mixed at the microscopic level and would exhibit a single glass transition temperature.[1]

Multiphase polymer blends are of high commercial interest due to the possibility of combining desirable properties. However, the positive enthalpy and low entropy of mixing generally associated with macromolecules often makes them immiscible with one another and they consequently phase separate.[1, 3] To alleviate this problem, a small amount of copolymer may be incorporated into the

blend to compatibilize the two phases.[4] The copolymer chains can be composed of one constitutive block miscible with one blend component and a second block miscible with the other blend component.[1] The presence of compatibilizer at the interface between the dispersed and continuous phases will prevent coalescence from occurring during subsequent processing, thus generating stable morphologies.[1] Compatibilizers can also be formed *in situ* at the interface between the two immiscible polymers by using homopolymers with reactive end groups in a process called reactive compatibilization.[5, 6] The main disadvantages of using premade copolymers is that is often difficult to diffuse through the bulk to the interface and the copolymers could become trapped in micelles in one of the homopolymer phases of the blend.[7] No such limitation exists for reactive blending and thus most commercial blends use this route (also pre-made block copolymers may be expensive to synthesize). The coupling of functional groups in reactive compatibilization is limited by thermal stability, reaction rates, the thickness of the interface and the elimination of small reaction by-products.[8] Some commonly used coupling reactions are amine-anhydride, amine-carboxylic acid, amine-epoxy, oxazoline-carboxylic acid, and epoxy-carboxylic acid.[8, 9] The thiol-epoxy reactive pairing has not been used in reactive compatibilization despite its success in industrial and biomedical applications.[10] The reaction is catalyzed by a variety of strong bases through deprotonation, and approach near quantitative yields when the appropriate catalysts are used. Even if the reaction rate is not sufficiently high, the thiol/epoxy pair could possess enough polar interactions for the effective physical compatibilization of the blend. An example

of a thiol-epoxy and an epoxy-carboxylic acid reaction can be seen in Figure 1 and 2 respectively.

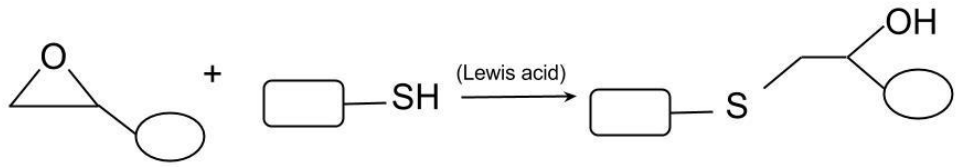

Figure 1Thiol-epoxy nucleophilic substitution reaction mediated by a Lewis acid[11]

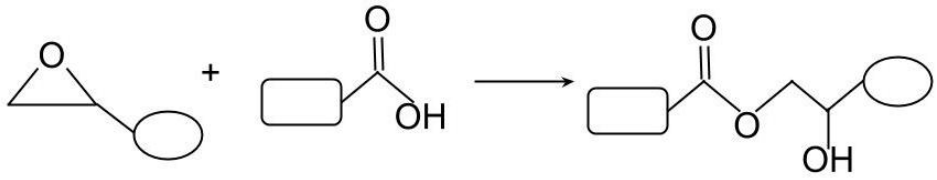

Figure 2 Epoxy-carboxylic acid esterification reaction[12]

Polymer Blends for Barrier Applications

Ethylene and propylene from petroleum-refining operations are relatively cheap raw materials for polymer production and are often used as the cost effective matrix, once polymerized into PE or poly(propylene), for polymer blending.[13] PE can be found in the production of gasoline tanks for automobiles due to its relatively low cost and desirable processing characteristics.[13] However PE containers have poor barrier properties for oily substances and need to be modified to have acceptable resistance.[14] For the modification of PE-based materials, it is paramount to use techniques that could be implemented industrially. Typically, PE-based fuel tanks have been processed with a relatively polar polyamide or polyester as the dispersed phase to enhance the resistance of PE tanks to hydrocarbon permeation.[13-15] The amine functionality of polyamides

and the carboxylic acid functionality of various polyesters make them ideal for blending applications with maleic anhydride and epoxy-grafted-PE, respectively.[16, 17] The addition of 20 wt.% of a polyamide to a PE matrix improves the permeability of the material by roughly 20 %,[18] but when the polyamide dispersed phase is reoriented in a lamellar morphology within the PE matrix the permeability becomes closer to that of a coextruded nylon sheet.[16] The improvement in barrier properties of the blend could be explained by the formation of a tortuous path by the dispersed polyamide phase that makes it difficult for the gasoline molecules to pass through.[16] The drawback of using polyesters or polyamides is that they are polymerized by condensation polymerization, resulting in polymers with relatively broad molecular weight distribution.[13] This means that more complex functionalities cannot be built into the barrier polymer (i.e. block copolymers) (eg. not only resistance to oil but resistance to moisture or oxygen). Thus, alternative barrier materials that can impart wider functionality due to more sophisticated microstructures are attractive. This thesis attempts to show one kind of alternative polymerization to make a candidate barrier material, by a controlled radical polymerization method termed reversible fragmentation transfer polymerization (RAFT).

Controlled Radical Polymerization

Polymerization is the process of joining together monomers by covalent bonds to produce long chain molecules. There are basically two approaches to polymer formation: chain and step growth polymerization. The former involves the addition of monomers to a single reactive site, which can be a cation, an anion

(ionic polymerization) or a radical (free radical polymerization), from which the polymer chain grows.[13] There are three essential stages for the formation of polymers through chain growth polymerization: initiation, propagation and termination. Initiation is the formation of an active center from where the chain starts to grow. Propagation involves the addition of more monomers to the growing chain end and termination is the disappearance of the active center and the stoppage of chain growth. Chain growth polymerizations are exemplified by radical polymerization, for example. In contrast, step-growth polymerization may have not only monomers adding to one another but larger molecules may react with one another, too. This method is used for the majority of polyesters, polyamides etc.

In 1956, Szwarc introduced the first "living" polymerization method through the ionic polymerization of styrene by electron transfer.[19] When using ions as the active centre in chain polymerization, the polymerization is considered to be living if there is no termination mechanism associated with the process and thus the polymerization can proceed indefinitely. A "living" polymer remains active, under the proper conditions, even after all the monomer has been consumed and upon the addition of more monomer, it would reactivate. The chain ends of a polymer made by such a mechanism remains sufficiently "living" that block polymers with well-defined structures and functionalities can be formed by the addition of a second, different monomer to the solution.[13] Ionic polymerization without termination using chain transfer reactions has been applied to a variety of monomers including methacrylates and styrene (ST).[20, 21] Even though ionic polymerization permits the formation of polymers with well-defined structures, it

requires rigorous purification of reactants and solvents, which generally makes it more expensive to implement in industry although in some cases products do exist that are made by ionic polymerization (the thermoplastic elastomer Kraton is one of such example). Radical polymerization, in contrast to ionic polymerization, can be carried out under more lenient conditions that can be easily scaled-up.[22, 23]

Radical polymerization, due to its versatility, has been used extensively in the production of high molecular weight polymers.[22] However, one of the problems associated with radical polymerization is its inability to form polymers with "living" characteristics. This limitation has been overcome over the past two decades with the emergence of controlled radical polymerization (CRP) techniques, which allows control over molecular weight distribution, end-group functionalities and architecture while maintaining the simple conditions of radical polymerization.[22] The most common CRP methods are nitroxide-mediated polymerization (NMP),[24] atom transfer radical polymerization (ATRP),[25-27] and RAFT[28-33]. It should be noted that other CRP methods have been developed such as reverse iodine transfer polymerization (RITP) and cobalt mediated radical polymerization (CMRP), which have not received as much attention as ATRP, NMRP and RAFT.[34, 35]

The polar nature of poly(acrylonitrile) (PAN) provides characteristics such as resistance to most chemicals and solvents, and low permeability toward gases.[36] However, PAN as a homopolymer is often difficult to compound since it is prone to thermal degradation.[36] Often AN is copolymerized with ST to improve its mechanical properties and to combine the desirable properties of both poly(styrene) PS and PAN into a single random copolymer such as poly(styrene-

ran-acrylonitrile) SAN.[36] SAN has been synthesized by the most common types of CRP: NMP,[24] ATRP,[25-27] and RAFT.[31, 33] Since the CRP techniques possess active centres, such centres are useful for post-polymerization modifications of the chain ends to impart functional groups. An example of such a chain end transformation is the focus of Chapter 2. A brief review of the major CRP processes is shown below, concluding with a discussion of the CRP method used in this thesis: RAFT.

Atom Transfer Radical Mediated Polymerization

ATRP, as proposed by Wang and Matyjaszewski in 1995, allows good control on the molecular weight and microstructure of polymers.[37] Control of the process comes from the equilibrium maintained between an active chain (P_n •) with *n* monomer groups and a dormant chain (P_n – X). The mechanism consists of a reduction/oxidation reaction between a dormant species which contains a carbon-halogen bond and a metal/ligand complex, such as copper (I) complexes with a ligand such as 2, 2-bipyridine, as illustrated in Figure 3. Several monomers are added during each activation step. If slow activation and a fast deactivation are maintained, transfer and termination reactions are mostly eliminated.[37] ATRP is a versatile process due to its ability to polymerize various monomers, including ST, AN, methacrylates, and acrylates.[38] ATRP also offers the possibility of functionalized polymers, and it is tolerant to many solvents, additives, and impurities.[26] Functionalized polymers using ATRP are accessible using functional initiators equipped with a radical stabilizing group on the carbon atom. Functional groups include aldehydes, amines, hydroxyl, phenyl, nitro, and

acids.[39] However, ATRP requires a metal/ligand catalyst, which needs to be removed at the end of the reaction.[25, 40] The concentrations of catalyst used in ATRP can be reduced by the use of active ligands tris[2-(dimethylamino)ethyl]amine and tris(2-pyridylmethyl)amine in a technique called Activators ReGenerated by Electron Transfer (ARGET). ARGET ATRP has been used to polymerize ST using low concentration of Cu/ligand catalyst complex which decreased the occurrence of catalyst-based side reactions and the problems associated with catalyst removal.[41]

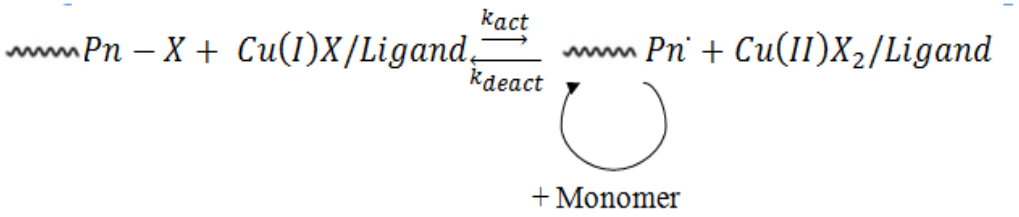

Figure 3 General mechanism for ATRP[40]

Nitroxide Mediated Polymerization

NMP was initially devised at CSIRO in the early 1980s[42] and was successfully utilized in the synthesis of ST-based polymers using 2,2,6,6-tetramethyl-1-piperidinyloxy, free radical (TEMPO) as initiator.[43, 44] Initially, NMP was limited to ST-based monomers and temperatures above 125 °C but with the development of acyclic nitroxides such as N-(2-methylpropyl)-N-(1,1-diethylphosphono-2,2-dimethylpropyl)-N-oxyl (SG1) and 2,2,5-trimethyl-4-phenyl-3-azahexane-3-oxy (TIPNO), the range of monomers polymerizable by NMP has increased to include AN,[45, 46] acrylates,[47] acrylic acid,[48] dienes,[49] and acrylamides.[50] The high activation-deactivation equilibrium constant of

methacrylates has made their NMP homopolymerization difficult; however, it was shown that the equilibrium constant in a SG1-mediated system can be significantly reduced by incorporating a small amount of ST as a co-monomer into a methyl methacrylate-rich mixture.[51, 52] The absence of post-polymerization catalyst removal in NMP greatly simplifies recovery procedures and is a good candidate to make SAN copolymers, especially considering that SAN polymerization by NMP has been previously reported.[53, 54]

Reversible Addition Fragmentation Chain Transfer

RAFT is compatible with the majority of monomers used in radical polymerization and tolerant to many functional monomers, solvents and initiators.[55] The first RAFT process reported in literature dates from 1996 where macromonomeric RAFT agents were utilized in the synthesis of polymers with narrow molecular weight distributions.[56] The use of dithiocarbonyl compounds to give living characteristics to radical polymerization was first reported by Chiefari et al. in 1998.[57] RAFT polymerization consists of the addition of a thiocarbonyl compound as the chain transfer agent (CTA) in addition to a conventional initiator such as azobis isobutyryl nitrile (AIBN) in a free radical polymerization system. Thiocarbonyl CTAs can be tailored to polymerize weakly or strongly activated monomers and during polymerization they establish equilibrium with the dormant chains and propagating radicals.[55] Switchable CTAs able to polymerized activated monomers such methyl acrylates (in the CTA's protonated form) and less activated monomers such as *N*-vinyl acetate (in the CTA's neutral form) are also available.[58] RAFT's ability to control a

polymerization is a reversible chain transfer step, unlike ATRP and NMP, which depends on a reversible termination step. Polymers obtained by RAFT are coloured and in some cases have strong odours due to the retention of the labile carbon-sulfur bond from the CTA.[59] Nevertheless, the removal of the end group has been shown to be effective at removing both colour and odour from the polymer chains.[59]

The key parameter of the RAFT polymerization is the addition-fragmentation equilibrium between the propagating radicals and the dormant polymeric thiocarbonyl compound.[22] The rapid equilibrium provides equal probability for all chains to grow simultaneously. The polymer chains retain the thiocarbonyl group and after the polymerization is stopped, may act as a macro-RAFT agent to chain-extend with another batch of monomer, thereby producing block copolymers potentially. Initiation, propagation, transfer and termination reactions occur as with conventional radical polymerization as illustrated in Figure 4. The mechanism in Figure 4 is generally accepted but there is still some debate on the kinetics of the RAFT process, especially the establishment of equilibrium and the possible side reactions that can complicate the process.[22] In an ideal RAFT process, the CTA behaves as a transfer agent, and therefore the kinetics of polymerization are not greatly affected by it.[22]

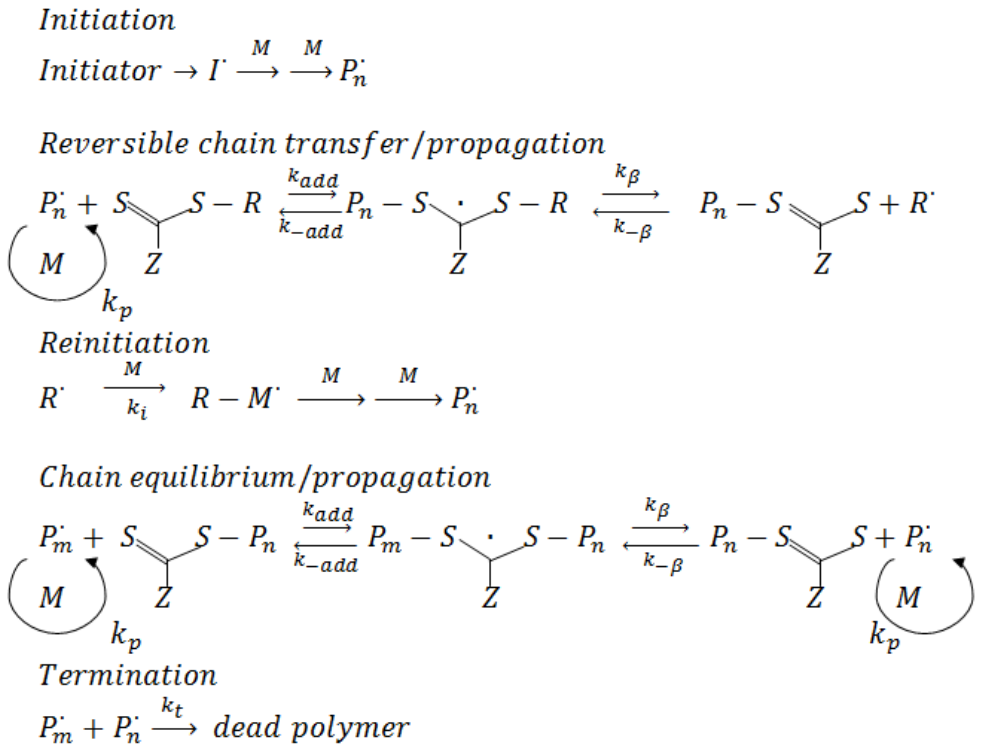

Figure 4 Mechanism of RAFT polymerization[60]

The effectiveness of the CTA depends on the monomer being polymerized and the properties of the free radical leaving group R, and the Z leaving group (Figure 5). Effective CTAs should have a thiocarbonyl group that must fragment rapidly in favour of products without side reactions and the radicals expelled should be able to reinitiate polymerization.[55, 61] Dithiobenzoates are among the most active agents for the polymerization of AN and ST monomers but they are sensitive to hydrolysis and decomposition by Lewis acids. Trithiocarbonate RAFT agents are generally a better option since they show less retardation and sensitivity to hydrolytic reactions.[55] The absence of catalysts and the presence of a trithiocarbonyl group in the chain after polymerization that could be modified to obtain functional groups, make RAFT a suitable technique for the development of

functional SAN polymers. Thus, the dibenzyl trithiocarbonate CTA was chosen for this study.

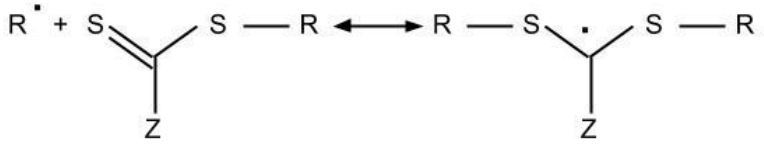

Figure 5 Structural features of thiocarbonylthio RAFT agent and the intermediate formed on radical addition. Z group modifies addition and fragmentation rates. R is a free radical leaving group and R' is free radical leaving group that is also to reinitiate polymerization.[62]

1.2 Research Objectives

The research presented in this thesis is divided in two sections: chapters 2 and 3. Chapter 2 consists of the application of RAFT techniques to synthesize thiol-terminated SAN (SH-SAN) to be blended with functional PE to make compatibilized blends via reactive blending. The RAFT technique was used to create SAN copolymers with low polydispersity index (PDI). In the present work only statistical SAN copolymers were prepared but RAFT permits the possibility of using microstructure copolymers to impart more sophisticated properties into barrier materials. SH-SAN was synthesized and melt blended with epoxy functional PE (E-PE). SH-SAN was obtained via an aminolysis reaction using butylamine. The compatibilization effectiveness of the blend between SH-SAN and E-PE was studied by comparing the morphology to a blend between SH-SAN and PE. The microstructures of these blends were characterized using scanning electron microscopy to determine the level of compatibilization achieved with the functional SAN by examining the size of the dispersed domains exemplified by

the volume-to-surface average diameter ($\langle D \rangle_{sv}$). The effect of unidirectional shear flow on the blend microstructure in the attempt to create a lamellar SAN morphology within the PE matrix was also investigated. Chapter 3 consists of the synthesis of epoxy functional SAN (E-SAN) by the terpolymerization of ST, AN, and epoxy functional glycidyl methacrylate (GMA) via RAFT. The subsequent ST/AN/GMA terpolymer was then to be used with a carboxylic acid functional PE (PE-COOH) in reactive blending experiments. This system was studied to increase the probability of acid/epoxy reactions by having more functional groups on each chain.

2 Synthesis of SH-SAN Copolymers for Reactive Blending with PE

2.1 Introduction

Blending is commonly use for the formation of barrier materials by blending a polyamide or a polyester in a polyolefin matrix such as PE.[13-15] Using simple melt blending and the incorporation of extensional flow fields in the die exit, a lamellar morphology of the dispersed phase is achieved, similar to the morphologies of multilayer materials, which require more capital-intensive die systems.[63] However, the positive enthalpy and low entropy of mixing generally associated with polymer blends require compatibilization to achieve a stable morphology at the operating conditions required for the application.[1] This can be alleviated by compatibilizers formed *in situ* through reactive blending processes.[5, 6] The inherent functionality of polyesters and polyamides, together with the use of functional polyolefins, permits reactive blending to take place.[17, 64] However, this is a limiting procedure towards using other materials which may be useful or better compared to poly(amides) or poly(esters).

PAN is known to have excellent barrier properties such as resistance to most chemicals and solvents, and low permeability toward gases.[36] However, PAN as a homopolymer can be challenging to process due to its high melt viscosity, high melting point, and poor thermal stability.[36] ST is commonly used as a comonomer with AN to improve the processability properties while maintaining the barrier properties associated with the AN units. The conventional free radical polymerization of SAN results in polymers with poorly defined microstructure and broad molecular weight distributions with PDIs ~2.[65] CRP can be used to

create SAN copolymers with low PDI and controlled microstructure, which allows additional tailoring of properties. SAN can be synthesized using the most common CRP techniques: NMP,[24] ATRP,[25-27] and RAFT.[31, 33]

SAN based copolymers are well known for their oxygen and carbon dioxide barrier properties and have important commercial applications due to their excellent chemical, thermal and mechanical properties, but they have not been applied widely in PE blends for barrier applications.[16] The main reason for this is the immiscibility of PE with SAN, which requires compatibilization in order to obtain a product with the desired, stable morphology. Reactive blending could be used for the compatibilization *in situ* of the blend by incorporating proper functionality to the blend components before the melt blending process.[5, 6]

During RAFT polymerization, the CTA that provides the control of the polymerization process is retained in the polymer chain and can be used to implement functionality to the polymer product.[61, 62] The thiocarbonyl group present in the polymer chain can be modified to produce thiol terminated resins via aminolysis or hydrolysis, which are colourless and odourless.[66-70] The thiol terminated polymers can be further reacted to obtain other types of functional groups[71]. Leaving the thiol group intact permits the reactive blending of the thiol-terminated polymer with polymers containing epoxy groups, which are easily grafted onto poly(olefins). Even though, the thiol-epoxy reaction has not been used in melt blending applications, it has been in the preparation of a variety of high molecular weight dual functional homopolymers as well as chain-end bifunctional oligomers.[10] The goal of this study was thus first to synthesize SH-SAN copolymers using RAFT and then melt blend the SH-SAN with E-PE to test

the effectiveness of the thiol-epoxy coupling to compatibilize the blend and produce a stable morphology. The resulting morphology was droplets and thus further processing to produce lamellar SAN domains in the PE was performed to obtain the desired morphology.

2.2 Experimental Section

Materials

ST (99%), and AN (99%) were purchased from Sigma-Aldrich and purified to remove the inhibitor by passing through a column of basic alumina (Brockmann, Type 1, 150 mesh) mixed with 5% calcium hydride (90– 95%, reagent grade), then sealed with a head of nitrogen and stored in a refrigerator until needed. Methanol (99.8%), hexane (98.5%), toluene (99.9%), chloroform ($CHCl_3$, 99.8%), tetrahydrofuran (THF, 99.9%), dimethylformamide (DMF, 99.8%) and triethylamine (Et_3N, 99%) were obtained from Fisher and used as received. Tris(2-carboxyethyl) phosphine hydrochloride (TPH), butylamine, and 5, 5-dithiobis(2-nitrobenzoic acid) (DTNB) were purchased from Sigma-Aldrich and used as received. Dibenzyl trithiocarbonate DBTC (97%) was purchased from Strem Chemicals Inc and used as received. 2, 2'-azobis(isobutyronitrile) (AIBN) (98%) was purchased from Sigma-Aldrich and purified by recrystallization from methanol. E-PE (trade name Lotader AX 8840) was obtained from Arkema and used as received. The E-PE was reported to have a melt flow index of 4.88 g/10 min (ASTM 1238/E) and a melting temperature of 100 °C. PS; ($\bar{M}_n$ = 13.0 kg mol^{-1}, PDI = 1.10) and PAN; ($\bar{M}_n$ = 60.6 kg/mol, PDI = 1.70) were used as

standards for Fourier transform infrared spectroscopy (FT-IR) and were obtained from Scientific Polymer Products Inc. Deuterated chloroform ($CDCl_3$, >99%) was purchased from Cambridge Isotopes Laboratory and used as received as solvent for ^{1}H NMR and ^{13}C NMR.

Synthesis of SAN using DBTC as CTA

A ST/AN RAFT copolymerization reaction in 50 wt.% DMF at 80°C was conducted using DBTC as CTA and AIBN as initiator. The polymerization was performed in a three-necked 25 mL round bottom flask equipped with a magnetic stirrer and a heating mantle/controller. A condenser connected to an ethylene glycol/water mixture recirculating chiller was attached to one neck of the flask to prevent the evaporation of the mixture components. The condenser was capped by a rubber septum with a needle to serve as an outlet for the nitrogen purge used. A thermal well attached to the temperature controller was connected to another port. The third port of the reactor was sealed with a rubber septum and was connected via a needle to a tank of nitrogen that supplied the purge to remove all oxygen from the reactor. AIBN (0.013 g) and DBTC (0.047 g) were first added to the reactor followed by DMF (10.81 g) and previously purified ST (8.00 g) and AN (2.73 g) ([Monomers]:[DBTC]:[AIBN] = 800:1:0.5). The reactor was sealed and then purged with nitrogen for 30 min. The reactor temperature was increased to 80°C at a rate of about 8.5ºC min^{-1} while maintaining the purge. When the temperature reached 80°C, the polymerization time was taken as the initial time. Samples were periodically removed and precipitated in methanol to allow kinetic data to be obtained. Typical polymerization times were about 360 min. The

reaction mixture was allowed to cool to room temperature. The aliquots were left to settle for several hours before the supernatant was decanted. The final polymer was precipitated in methanol three times, vacuum filtered, and then dried overnight in a vacuum oven at 50°C to thoroughly remove any solvent and unreacted monomers from the samples. The initial AN molar composition ($f_{w,}$ w = monomer) was 0.40, which is near the copolymer composition azeotropic point.[31] The target $\bar{M}_n$ at complete conversion, calculated by the mass of monomers relative to the moles of DBTC, was set to 66 kg·mol^{-1}. After the aminolysis reaction the 66 kg·mol^{-1} target $\bar{M}_n$ will convert into a value slightly above the critical molecular weight ($\bar{M}_{n,c}$) for PS ($\bar{M}_{n,c}$ at 140 °C = 26 kg·mol^{-1}) which should enhance entanglement (aminolysis should yield a product with half the molecular weight of the parent polymer).[4] The final yield after 366 min for this particular sample was 5.36 g (50 % conversion of monomers based on gravimetry). The SAN polymers used in this study together with their corresponding $\bar{M}_n$s and PDIs are listed in Table 1. The AN molar composition of the comonomer was found to be 0.40 using both FT-IR and ^{13}C NMR. The FT-IR absorbance at 700 cm^{-1} and that at 2240 cm^{-1} were used as markers for ST and AN, respectively. For ^{13}C NMR, the quaternary carbon resonance values for the ST residue at 146.4–138.7 ppm and the nitrile carbon resonance of the AN residue at 122.5–117.5 ppm were used markers for the determination of AN content.

Table 1 Characteristics of the ST/AN Copolymers

Experiment ID[a]	$\bar{M}_n$ (kg·mol^{-1})[b]	PDI[b]	AN content (%)
SAN-31	37.6	1.31	40
SAN-40	31.3	1.31	35
SH-SAN-33	27.4	1.34	40
SH-SAN-44	27.0	1.35	35

[a]Experimental ID is given by the following notation SAN/SH-SAN-xx where xx represents the experiment number

[b]$\bar{M}_n$s and PDIs were determined by gel permeation chromatography calibrated relative to linear PS standards in THF at 35 ºC

The theoretical $\bar{M}_n$ ($\bar{M}_{n,th}$) was calculated using the following equation (Equation 1):

$$\bar{M}_{n,th} = \frac{[ST] \cdot M_{ST} \cdot f_{\mathrm{ST}} + [AN] \cdot M_{AN} \cdot f_{\mathrm{AN}}}{[DBTC]_0} \cdot x + M_{DBTC}$$

Equation 1

where [ST], [AN] and [DBTC] are the initial concentrations of ST, AN and DBTC, M_{ST}, M_{AN} and M_{DBTC} are the molecular weights of ST, AN and DBTC, respectively and x is conversion. This equation assumes an ideal RAFT system where the polymers directly derived from the initiator are thought to be minimal.[32]

Thiol Functionalization of SAN through an Aminolysis Reaction

The functionalization of SAN prepared by RAFT polymerization was accomplished by the conversion of the trithiocarbonate to thiol groups through an aminolysis reaction (Scheme 1). SAN-31 (2.0 g) was dissolved in 20 mL of

anhydrous toluene followed by the addition of a small amount of the reducing agent TCEP (catalyst amount). The mixture was then purged with dry nitrogen for 30 min in a 125 mL single-neck glass round bottom flask. The flask was sealed with a rubber septum, and was fitted with a needle to relieve pressure. A 50-fold molar excess of n-butylamine (0.44 mL) was added to the solution. The mixture was stirred for 300 min at room temperature while purging with dry nitrogen. SH-SAN was isolated by precipitation of the reaction mixture into methanol and dried in a vacuum oven at room temperature for 24 h. The SH-SAN-33 final product $\bar{M}_n$ and PDI determined by GPC calibrated relative to linear PS standards in THF at 35ºC and are reported in Table 1.

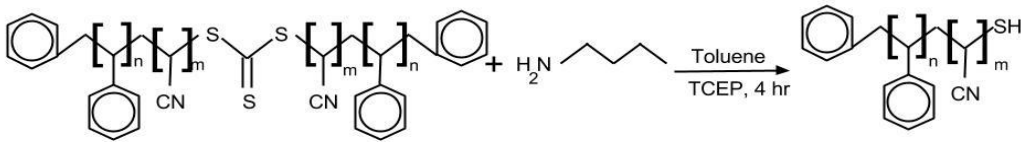

Scheme 1 Aminolysis reaction of SAN and butylamine in the presence of TCEP to produce SH-SAN

The outcome of the aminolysis reaction was assessed by visible ultraviolet spectroscopy (UV-vis) using the characteristic absorbance centered at 310 nm of the trithiocarbonate group (ε_{310nm} = 14300 M^{-1} cm^{-1} in $CHCl_3$) by looking at the spectra of $CHCl_3$ solution of SAN and SH-SAN of identical concentration (1.0 mg $\cdot$ mL^{-1}).[66]

Ellman's Assay

The presence of the thiol end-group in SH-SAN was studied by a modified Ellman's method as shown in Scheme 2.[72, 73] In the presence of Et_3N, the thiol-containing polymer was reacted with DTNB in DMF, and the resulting 2-nitro 4-

thiobenzoate dianion (NTD) was detected by its absorbance at 501 nm (ε_{5O1} 24 400) (Scheme 2). The details were as follows: 3.0 mg of finely divided SH-SAN-33 was suspended in 15 mL dry DMF under nitrogen at 25°C for 1 h, followed by the addition of DTNB and Et_3N at the following ratio: [SH]/[DTNB]/[Et_3N] = 1/5/100. The reaction mixture was shaken in the dark at room temperature for 15 min before the absorbance at 501 nm was recorded using UV-vis. A mixture of Et_3N, DTNB and dry DMF was used as blank.

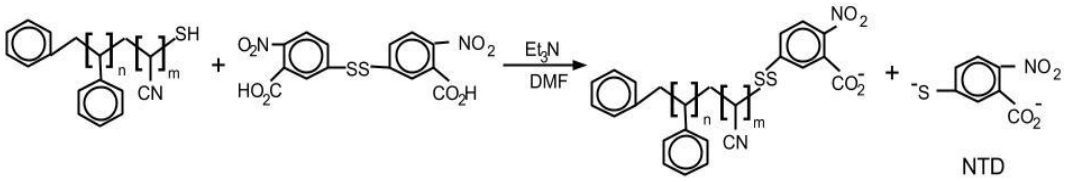

Scheme 2 SH-SAN reaction with DTNB in the presence of Et_3N to produce NTD

Melt Rheology of SH-SAN and E-PE

E-PE sample discs of 25 mm diameter and 1 mm thickness (0.6 g) at 160°C and 10 tons clamping force between poly(tetrafluoroethylene) sheets in a Carver model 3857 hot press. The clamping force was kept constant for 30 minutes with only quick pressure releases every ten minutes to remove any gas bubbles. The discs were cooled by water-cooling the plates at a rate of 40°C·min^{-1} while keeping the clamping force at 12 tons. The same procedure was used to make SH-SAN-40 discs but the operating temperature was reduced from 160°C to 120°C. The E-PE and SH-SAN-40 sample disks were placed in an Anton Parr MCR302 parallel plate rheometer and a frequency sweep experiment at 180°C was

performed. To remain within the linear viscoelastic regime, the strain was kept below 10%. Angular frequency was varied between 1 and 100 s^{-1}.

Melt Blending of SH-SAN and E-SAN

SH-SAN was melt blended with a previously made E-SAN copolymer with 6 wt.% GMA content to evaluate the reactivity of the thiol/epoxy reaction using GPC. This was done to estimate the effect of reaction for the blend of interest, E-PE/SH-SAN since there is no common solvent available for PE and SAN. SH-SAN-44 (0.50 g) and E-SAN (0.22 g) were mechanically blended at room temperature, and then fed into a miniature twin screw extruder (Haake Minilab) at 180°C operated at a screw speed of 150 rpm. The material was in the extruder for 5 minutes and then scraped off the screws since there was not enough material exiting of the extruder. The material was quenched in liquid nitrogen after it was removed from the screws to ensure that the morphology was frozen. The polymers were characterized using GPC against linear PS standards at 35°C in THF.

Melt Blending of SH-SAN Copolymer and PE

SH-SAN-33 (0.55 g, 20 wt.% in E-PE) and E-PE (2.2 g) were mechanically mixed at room temperature, then fed into a miniature twin screw extruder at 180°C operated at a screw speed of 150 rpm. The material was in the extruder for 12 minutes and then immediately quenched in liquid nitrogen to ensure that the morphology was frozen. The same procedure was followed for the blending of SH-SAN-33 with PE. Electron microscopy was used to determine the blend morphology (see section on sample preparation below for more details). Samples

were also annealed under vacuum at the blending temperature (180°C) (above the glass transition temperatures of SH-SAN and E-PE) for 20 min to determine the morphological stability of the reactive and non-reactive blends.

Reorientation of SAN Domains Using a Channel Die

The SH-SAN-33/E-PE blend was subjected to unidirectional reorientation within a channel die similar to what has been described in the literature.[74, 75] The channel was 6 mm wide by 15 mm deep by 60 mm long (Figure 6). SH-SAN-33/E-PE blend samples of 0.14 g each were first pressed into a rectangular shape 6 mm by 15 mm by 2 mm to ensure unidirectional flow within the channel die (Figure 7). Figure 7 also illustrates the possible streamlines within the channel die assuming: the polymer behaves as an uncompressible viscous liquid; the flow is fully developed and laminar; and no-slip conditions prevail. The channel die was heated between the two platens of the hot press at 180°C. The rectangular piece of SH-SAN-33/E-PE blend was put in the centre of the channel making sure that the polymer fit tightly into the channel die, and the plunger was placed on top of the die. The platens were closed carefully and held for 1 min. Then the platens were pushed together at a constant rate until polymer ribbons were extruded from both ends of the channel. The applied clamping force did not exceed 6 tons. The polymer ribbons were removed gently with tweezers and immediately quenched in liquid nitrogen to ensure that the morphology was not further altered.

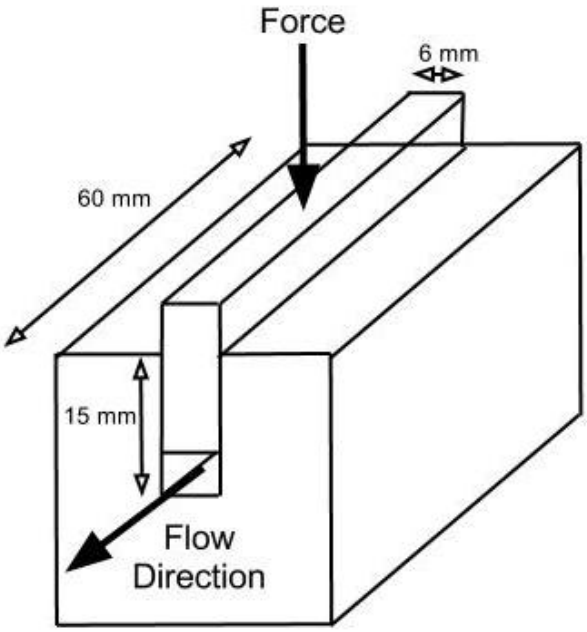

Figure 6 Diagram of the channel die and the direction of polymer flow and applied force[75]

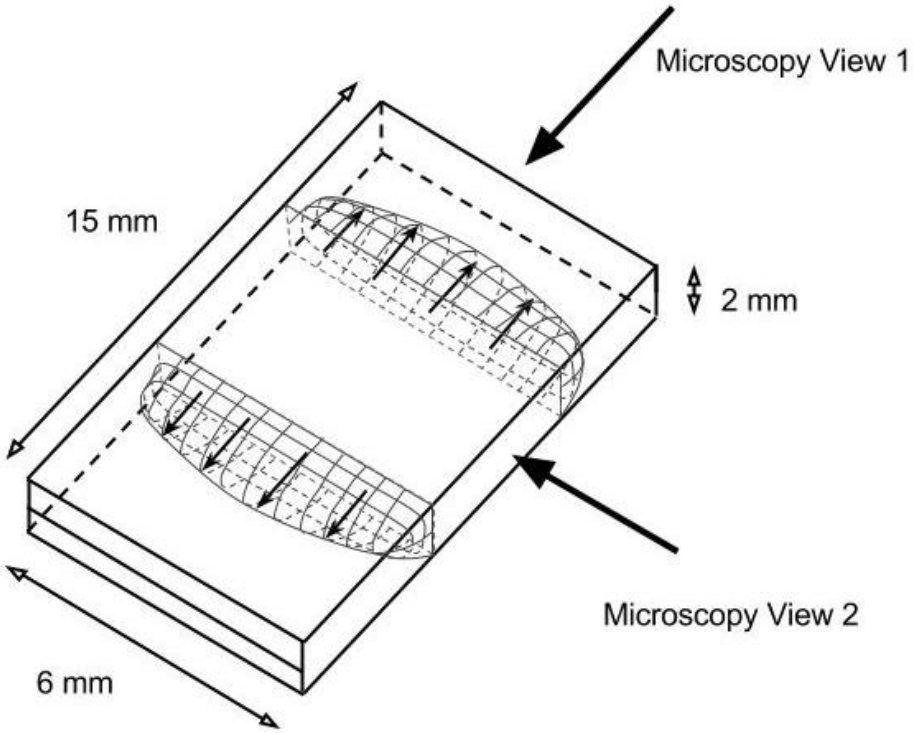

Figure 7 Diagram of the rectangular shaped polymer for reorientation, microscopy views, and possible streamlines[75]

Sample Preparation for Microscopy

For the SH-SAN-33/E-PE and the SH-SAN-33/PE blends, quenched samples were freeze fractured in liquid nitrogen and after thorough drying the samples were placed in THF for 4 hours to selectively remove the dispersed SAN phase. The samples were then glued onto aluminum stubs and sputter-coated with 20 Å of Au-Pd to make the sample conductive. The imaging of the samples was performed using an Environmental Scanning Electron Microscope (ESEM, FEI Co.) equipped with a field emission gun, at an accelerating voltage of 20 kV.

Image Analysis

The particles were traced onto a transparency and scanned at a resolution of 300 dpi to ease the determination of the dispersed phase drop size, which was performed using Image J Version 1.45s software. The areas were converted to an equivalent sphere diameter, where at least 300 particles were counted from each sample to ensure reliable statistics. The size of the dispersed phase was characterized by the $\langle D \rangle_{sv}$, which gives the average interfacial area per unit volume. $\langle D \rangle_{sv}$ can be used to determine how much graft copolymer is formed at the polymer/polymer interface.[76]

Characterization

Molecular weights ($\bar{M}_n$, $\bar{M}_w$) and PDI were estimated using GPC (Waters Breeze) with THF as the mobile phase at a flow rate of 0.3 mL·min^{-1}. The GPC was equipped with three Styragel® HR columns (HR1 with molecular weight

measurement range of 10^2 to 5×10^2 g·mol^{-1}, HR2 with molecular weight measurement range of 5×10^2 to 2×10^4 g·mol^{-1} and HR4 with molecular weight measurement range of 5×10^3 to 6×10^5 g·mol^{-1}) and a guard column. The columns were kept at 35°C during the analysis and the molecular weights were estimated relative to linear PS standards. The GPC was equipped with both differential refractive index (RI 2410) and ultraviolet (UV 2487) detectors for which the RI detector was used solely for the experiments described herein.

Attenuated total reflectance (ATR) Fourier transform infrared spectroscopy (Spectrum BX, Perkin-Elmer) was used to determine the molar compositions of the SAN copolymers. An ATR correction was used on the spectra. The absorbance at 700 cm^{-1} and that at 2240 cm^{-1} were used as markers for ST and AN, respectively. To precisely identify the copolymer compositions, 6-point calibration curves were constructed with mixtures of PS and PAN standards, Figure 8. This has been shown to be a relatively effective way to determine SAN copolymer composition.[77]

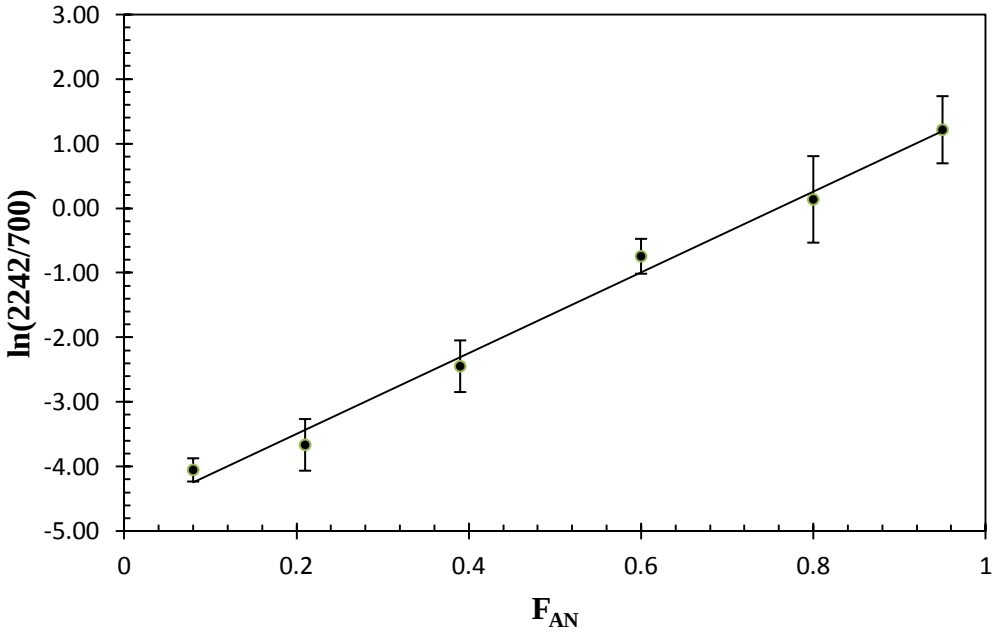

Figure 8 Calibration curve constructed using FT-IR with mixtures of PS and PAN standards for the purpose of determine the composition of the copolymers. The y-axis represented the natural logarithm of the ratio between the FT-IR absorbance at 2242 cm^{-1} (PS absorbance) and 700 cm^{-1} (PAN absorbance) of mixtures of PS and PAN at different molar concentrations

To better establish the AN composition, ^{13}C NMR was performed with a 500 MHz Varian Mercury instrument by doing a total of 1024 scans on each sample. The quaternary carbon resonance values for the ST residue at 146.4–138.7 ppm and the nitrile carbon resonance of the AN residue at 122.5–117.5 ppm were used for the determination of the ST and AN polymer content.[78]

UV-vis (CARY 5000 spectrophotometer from Varian) was used to determine the effectiveness of the aminolysis reaction by tracking the absorbance of the trithiocarbonate group in $CHCl_3$ in wavelengths ranging from 250 to 400 nm. UV-vis was also used to verify the presence of thiol groups in the polymer by measuring the absorbance of NTD in $CHCl_3$.

Thermal gravimetric analysis (TGA; Q500 from TA Instruments) was used to determine the thermal stability of SH-SAN and E-PE. The temperature was increased at 20°C·min^{-1} from 25°C to 700°C.

Differential scanning calorimetry (DSC; Q2000 from TA Instruments) was used to determine the glass transition temperature and the melting temperature of the polymers. A heat, cool, heat cycle was done with a temperature range of -90°C to 200°C. The measurements from the second heat cycle were used for the analysis since the first cycle was performed to remove any thermal history. The DSC was calibrated using indium standards for enthalpy.

2.3 Results and Discussion

SAN Polymerization by RAFT

The copolymerization of ST and AN using controlled radical polymerization was performed by RAFT using DBTC as chain transfer agent and AIBN as initiator. The synthesis of SAN using DBTC has not being reported before. However, DBTC was used to synthesized separately the homopolymers of PS and PAN separately.[32, 79] The copolymerization of ST and AN afforded poly(styrene-*ran*-acrylonitrile) with trithiocarbonate units in the middle of the SAN chain since the growing chain can propagate in both sides of DBTC. The kinetic plot of the copolymerization exhibited a linear evolution during the first 200 min of polymerization after which a plateau is reached (Figure 9). The slope calculated, typically from about four to five sample points taken in the linear region, from such plots reveals the apparent rate constant. The apparent rate constant was 0.003

min^{-1}, which was similar to PS polymerizations performed by the author under similar conditions and other SAN polymerizations by RAFT found in literature.[31] The polymerizations also exhibited some linearity in the evolution of $\bar{M}_n$ with conversion (Figure 10), which suggests a controlled polymerization. Figure 10 also showed that at zero conversion the $\bar{M}_n$ is ~10 kg·mol^{-1}; this discrepancy could be explained by polymer formation before the system reached 80ºC. $\bar{M}_n$ dependence versus conversion was not linear for conversion values higher than 40-50%. Nevertheless, preparation of polymers with PDI = 1.3-1.4 and $\bar{M}_n$ of 31.4-37.6 kg·mol^{-1} was possible. PDIs change with increasing conversion in the range of 1.28-1.34 typical for RAFT-prepared copolymers and were well below the theoretical lower limit of 1.50 for a normal free radical polymerization.

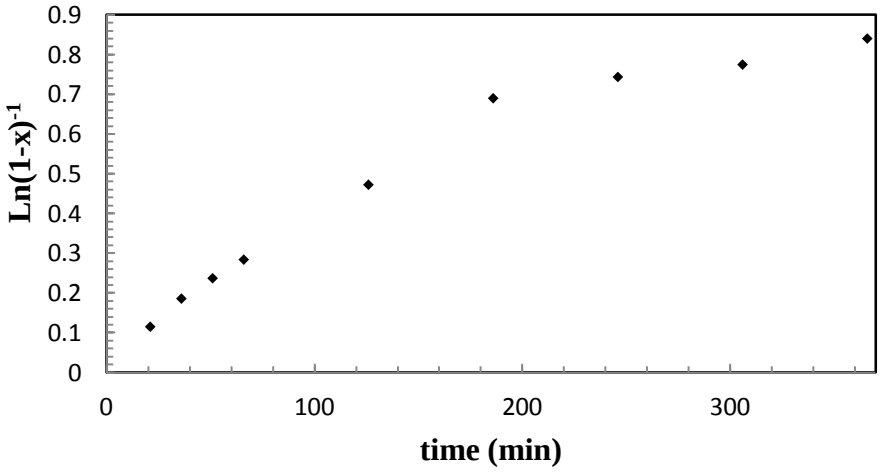

Figure 9 Semi-logarithmic kinetic plot ln[(1-x)$^{-1}$] (x = monomer conversion) versus polymerization time for typical ST, AN copolymerizations in DMF at 80°C in the presence of DBTC as CTA and AIBN as initiator.

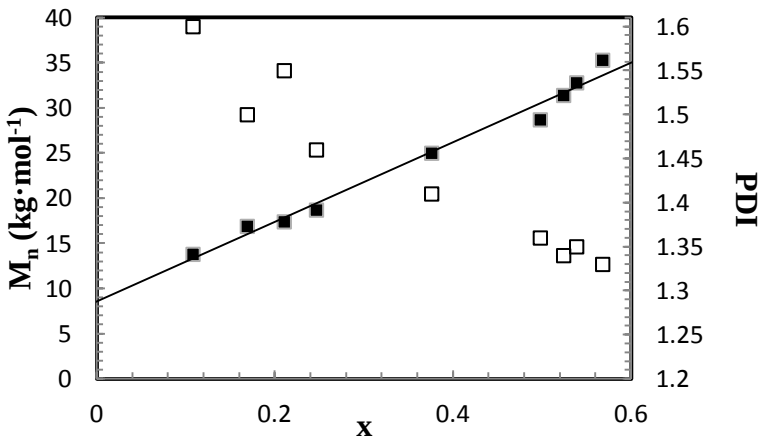

Figure 10 $\bar{M}_n$ and PDI as a function of x for a typical copolymerization of ST and AN by RAFT using DBTC as CTA and AIBN as initiator in DMF at 80°C. The straight solid line indicates the theoretical $\bar{M}_n$ against x based on the monomer to CTA ratio. [Monomer] = 50 wt.%, [ST]/[AN] = 60/40, and [monomer]/[DBTC]/[AIBN] = 800/2/1. $\bar{M}_n$ is indicated by the filled squares (■) and PDI is indicated by the open squares (□).

The composition of SAN was determined by FT-IR spectra and ^{13}C NMR. FT-IR peak absorbances at 700 cm^{-1} and 2240 cm^{-1} were used as markers for ST and AN, respectively. The AN content of SAN for the polymerizations was found to be between 32-40%. ^{13}C-NMR was also employed to determine the AN content in the polymer. Figure 11 shows the ^{13}C NMR spectra of a SAN-31 polymer where the AN content was found to be 40%. The composition calculated with ^{13}C NMR was consistent with that calculated using FT-IR.

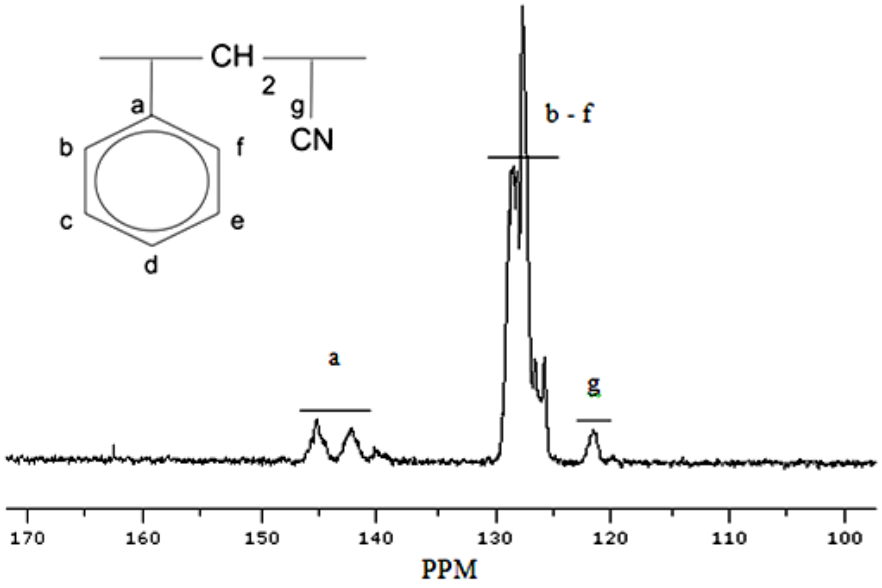

Figure 11 ^{13}C NMR spectra of SAN-31 (solvent $CDCl_3$)

Thermal Stability of Polymers

Since the SH-SAN-33 and E-PE were to be blended in an extruder at 180°C, it was important for them to be thermally stable. TGA was performed on SH-SAN-33 and E-PE (Figure 12). At 180°C, 97% of SH-SAN-33 and 100.0% of the E-PE remained. This indicates that the blends should be relatively stable at the processing temperatures used.

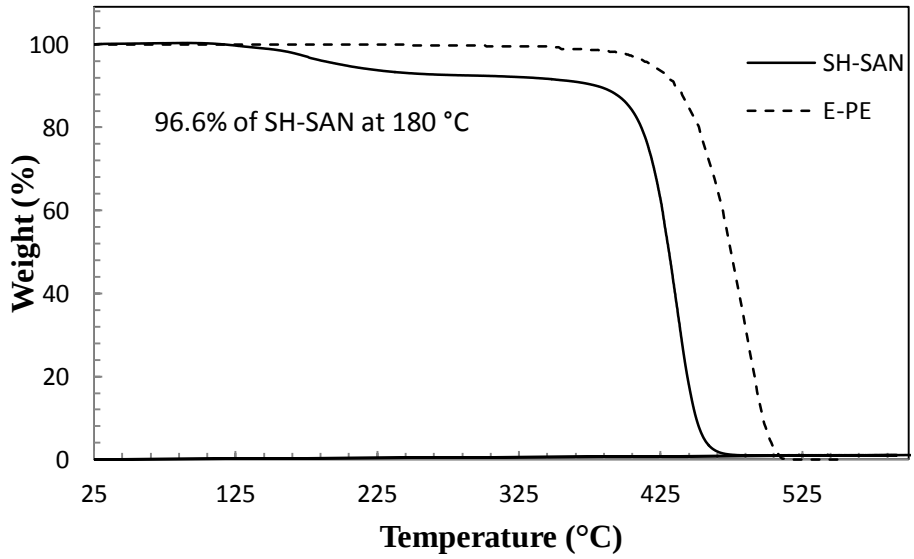

Figure 12 TGA of SH-SAN-33 and E-PE

End-group Modification of SAN

The functionalization of SAN prepared by RAFT polymerization was accomplished by the conversion of the trithiocarbonate located in the middle of the chain to thiol groups through an aminolysis reaction with butylamine. The reaction was performed in the presence of TCEP to inhibit the formation of disulfide coupled polymers. The originally yellow SAN-31 turned white; this change in colour is a good indication of the formation of SH-SAN-33.[80] FT-IR was used to observe the formation of a new peak in the SH-SAN-33 spectrum (thiol groups absorption is located in the 2550-2600cm^{-1} range). However, perhaps due to the low concentration of end groups on the long polymer chain, the appearance of thiol end groups using FT-IR was difficult to observe. The outcome of the aminolysis reaction was assessed also by UV-vis. As seen in Figure 13, the UV-vis spectra of $CHCl_3$ solution of SAN-33 exhibits a strong absorption

centered at 310 nm while only a weak absorption can be detected in this spectral region for SH-SAN-33.

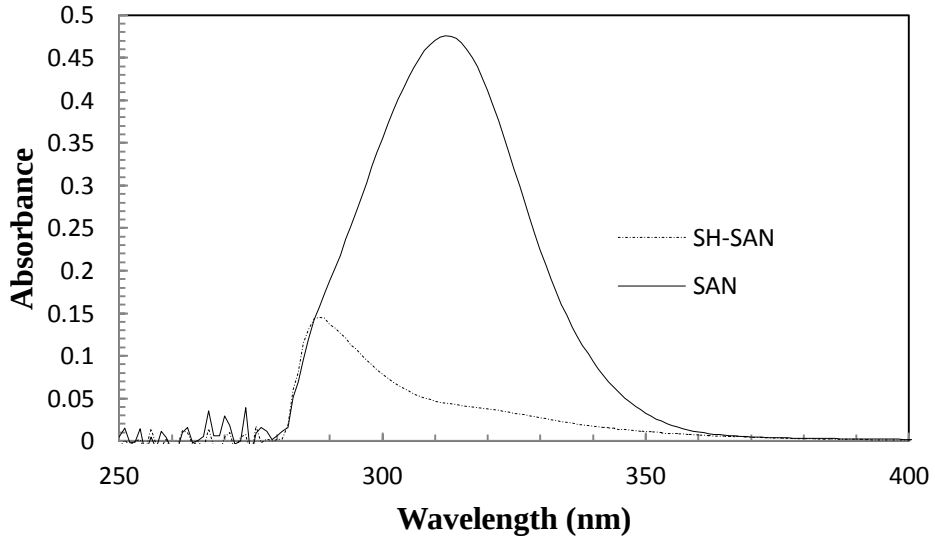

Figure 13 UV-vis spectra of the precursor polymer SAN-31 (solid line) and the aminolyzed polymer SH-SAN-33 (dashed line).

The $\bar{M}_n$ was expected to halve from SAN-31 to SH-SAN-33 due to the formation of two thiol terminated chains from the parent trithiocarbonate-containing polymer.[79] The GPC plot in Figure 14 shows the results of the aminolysis reaction. The peak of the SH-SAN-33 appeared at higher elution time than the parent SAN-31 polymer, indicating that a polymer with lower $\bar{M}_n$ was formed after the aminolysis reaction. The $\bar{M}_n$ went down from 37.6 kg·mol^{-1} (SAN-31) to 27.4 kg·mol^{-1} (SH-SAN-33) after the aminolysis reaction while the PDI increased only slightly from 1.31 (SAN-31) to 1.34 (SH-SAN-33). Even though the $\bar{M}_n$ of the thiol terminated polymer was lower than the parent polymer, it was not exactly half. This could be due un-reacted parent chains or by the formation of disulfide linkages between thiol terminated chains.

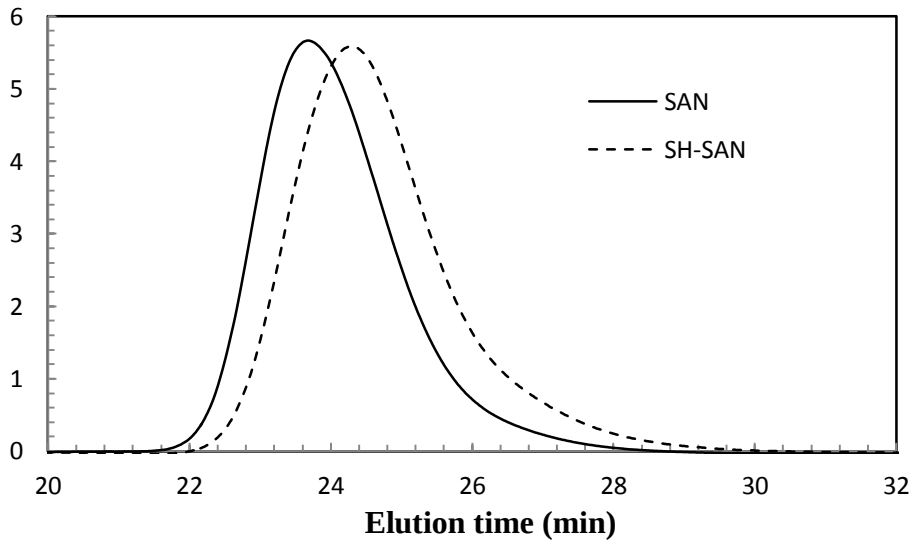

Figure 14 GPC results for the aminolysis reaction of SAN-31 (solid line) using butylamine and the product SH-SAN-33 (dashed line)

The presence of thiol groups in the polymer was examined using a modification of Ellman's method by observing the characteristic absorbance of the product 2-nitro 4-thiobenzoate dianion (NTD) of the reaction between SH-SAN-33 and DTNB.[72] NTD exhibits a characteristic absorbance centered at 501 nm and only forms if there are thiol groups to react with (Scheme 2). Figure 15 shows the UV-vis spectra of the reaction mixture of SH-SAN-33 and DTNB in the presence of triethylamine (Et_3N) and using DMF as solvent, before and after adding DTNB. Figure 15 shows that after adding DTNB, a strong absorption centered at 501 nm emerges confirming the presence of thiol groups in SH-SAN-33. The absorption at 501 nm confirms the formation of NTD, which is the product of the reaction between the thiol groups of SH-SAN-33 and DTNB.

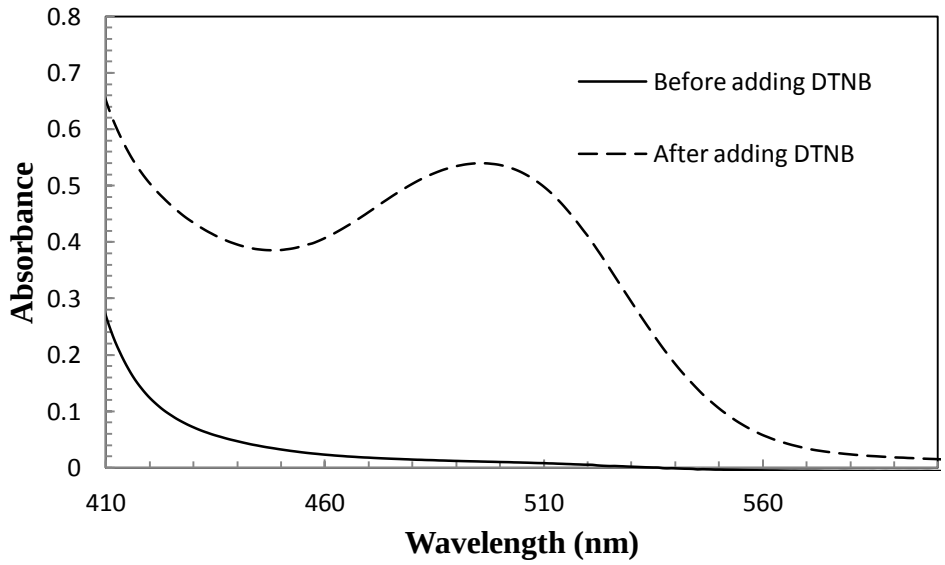

Figure 15 UV-vis spectra of the reaction mixture of SH-SAN-33 and DTNB in the presence of Et_3N and using DMF as solvent, before and after the addition of DTNB.

Rheology of SH-SAN, E-PE and PE

Complex viscosity measurements for SH-SAN-44, E-PE and PE are shown in Figure 16 against varying angular frequency. The maximum shear rate was calculated by dividing the linear screw speed by the gap distance:

$$\dot{\gamma}_{max} = \frac{\pi N D_{top}}{G}$$

where $\dot{\gamma}_{max}$ is the maximum shear rate, D is the screw diameter, N is the rotation rate and G is the gap distance. The maximum shear rate, which occurs at the top where the screws are widest and has the highest linear velocity, was found to be approximately 80 s^{-1}. The D_{top}, D_{bottom} and G dimensions and N of the extruder at the top were approximately 10 mm, 3.5 mm, 1 mm and 150 rpm. Assuming the Cox-Merz rule applies, the steady shear rates in the extruder were matched to the frequencies shear rates in the rheometer. The Cox-Merz rule states that oscillatory

experiments are identical to steady shear viscosity.[81] Therefore, the viscosity inside the extruder was approximated using the rheological measurements at 180°C and angular frequency of 80 s^{-1}, which is the maximum shear rate within the extruder. At these conditions, the complex viscosities of the E-PE, PE, and SH-SAN-44 were 400 Pa·s, 200 Pa·s and 50 Pa·s, respectively. The viscosity ratios of the dispersed phase (SH-SAN-44) to the matrix phase (PE/E-PE) for the SH-SAN-44:E-PE blend and the SH-SAN-44:PE blend were 0.12 and 0.25, respectively. The closer the viscosity ratio is to unity, the better the mixing and the smaller the dispersed phase particle size.[82-84] However, interfacial tension and elasticity also play a role in the mixing which could affect the dispersed particle size.[85]

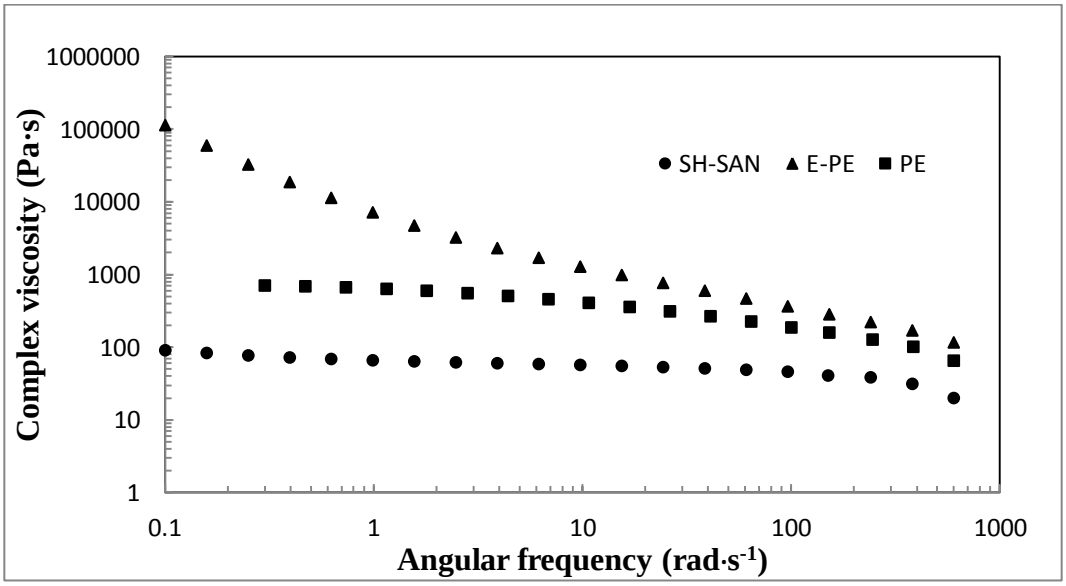

Figure 16 Complex viscosity measurements of SH-SAN-44, E-PE and PE at 180 °C obtained using a parallel plate rheometer.

Melt Blending of SH-SAN and E-SAN

The SH-SAN-33 and SAN polymers were melt blended with E-SAN copolymer to evaluate the reactivity of the thiol-epoxy reaction under homogeneous conditions. This would suggest how effective the reaction would be for heterogeneous PE/SAN blends. In the latter case, GPC is not possible since there is not common solvent for the PE-SAN system. The presence of the reaction was evaluated by GPC and the results are presented in Figure 17. The elution time peak of the blend shows no difference from the peaks of the individual polymers, indicating that no reaction occurred. The blend shows only a single elution time peak which corresponds to the overlap between the SH-SAN-33 ($\bar{M}_n$ = 27.4 kg·mol^{-1}, PDI = 1.34) and E-SAN ($\bar{M}_n$ = 34.8 kg·mol^{-1}, PDI = 1.48). The blend coupled peak is closer to that of SH-SAN-33 possibly because the SH-SAN-33 loading in the blend was higher. These results suggest that a catalyst is needed to enhance the reaction between the thiol and epoxy groups in the SH-SAN-33 and E-SAN respectively.

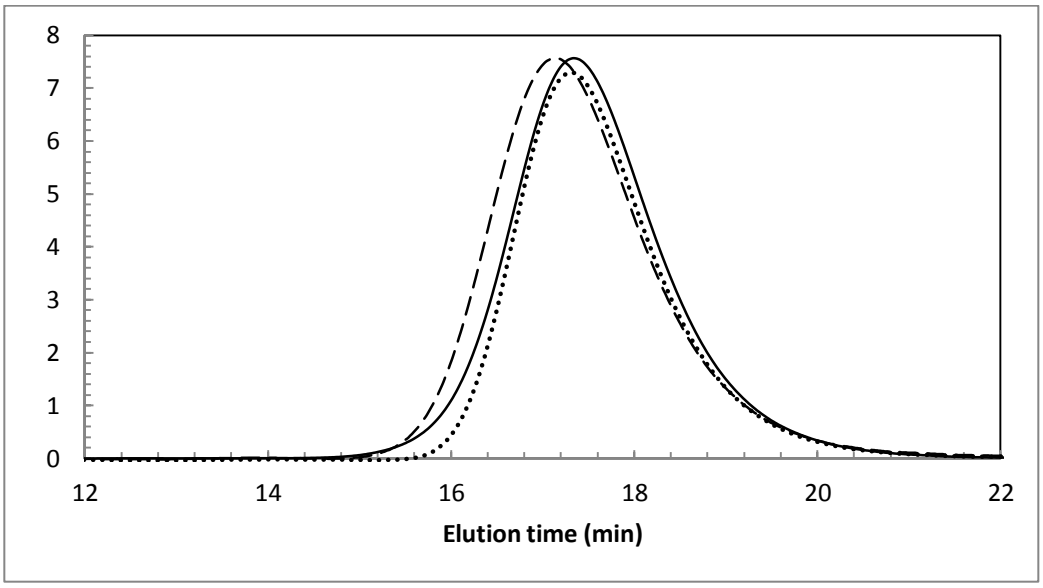

Figure 17 GPC results for SH-SAN-33 (dotted line), E-SAN (dashed line), and the blend between S-SAN and E-SAN (solid line).

Melt Blending of SH-SAN/E-PE and SH-SAN/PE

The SH-SAN-33/E-PE and SH-SAN-33/PE blends were separately mixed in a miniature twin extruder at 20 wt.% SAN (the minor phase) loading, which is common for PE blends for barrier applications.[18] ESEM images of the blends are shown in Figure 18 and a summary of the morphology characterization is presented in Table 2. $\langle D \rangle_{sv}$ for the SH-SAN-33/E-PE blend was 1.3 μm, while $\langle D \rangle_{sv}$ for the SH-SAN-33/PE blend was 3.7 μm. This indicates that the SH-SAN-33/E-PE blend was able to prevent dynamic coalescence better compared to the SH-SAN-33/PE blend. The difference in particle size could be explained by the interaction between the thiol groups in SH-SAN-33 with the epoxy groups in E-PE. The thiol/epoxy interaction could have formed a copolymer at the interface between the immiscible phases. Considering that the SH-SAN-33/E-PE blend showed a smaller particle size than the SH-SAN-33/PE blend despite having a viscosity ratio farther away from unity (0.12 compare to 0.25), it is plausible that come sort of compatibilizing effect was present.[86] Similar blends of non-functional SAN showed a 50% increase in particle diameter when the viscosity ratio changed from 0.21 to 0.16.[86]

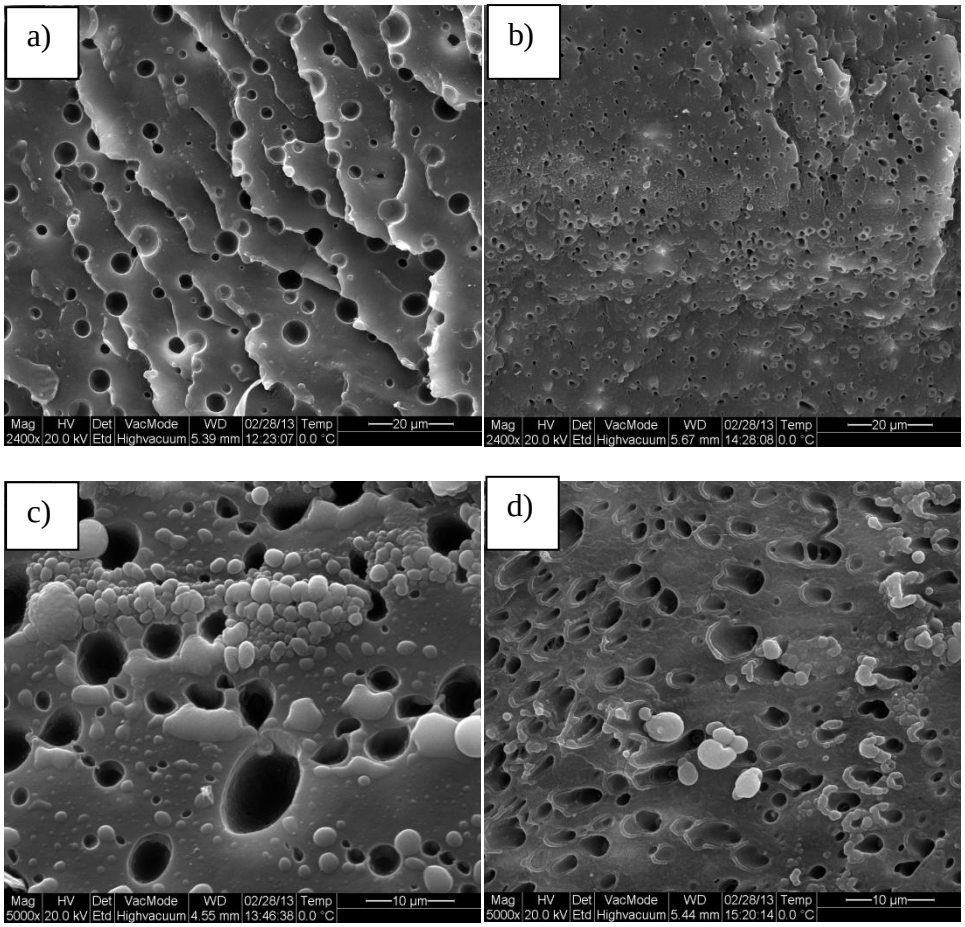

Figure 18 ESEM images of a) SH-SAN-33/PE (20/80) after extrusion and freeze-fracturing, b) SH-SAN-33/E-PE (20/80) after extrusion and freeze-fracturing, c) SH-SAN-33/PE (20/80) annealed at 180°C for 20 min and d) SH-SAN-33/E-PE (80/20) annealed at 180 °C for 20 min. The SAN phase was removed by etching with THF to show contrast between the phases.

To test the stability of the blends, thermal annealing was done on the samples at the extrusion temperature (180°C) for 20 min, which should be sufficient to observe static coalescence effects.[85] The annealing temperature was above the melting point of both polymers. $\langle D \rangle_{sv}$ of the annealed blends are also reported in Table 2. There was coarsening of the morphology during the annealing process in the SH-SAN-33/E-PE blend as the $\langle D \rangle_{sv}$ doubled. The coarsening of the non-reactive SH-SAN-33/PE blend was not as notable as in the SH-SAN-33/E-PE

blend. The slow coarsening exhibited by the non-reactive blend could be a consequence of both the annealing time (20 min) and temperature (180ºC). The non-reactive blend did not have sufficient time to have coarse completely at the annealing temperature used. The annealing results show that thiol/epoxy interactions in the SH-SAN-33/E-PE blend were not stable and upon annealing coarsening occurred. Nevertheless, the SH-SAN-33/E-PE blend consistently gives a smaller $\langle D \rangle_{sv}$ than the SH-SAN-33/PE blend despite having a lower viscosity ratio. Based on these results, the thiol/epoxy coupling did contribute to a compatibilizing effect but did not lead necessarily to a stable morphology, under the annealing conditions used. Another possible reason for the increase in drop size for the reactive blend after the annealing is the possible degradation of the SH-SAN-33 which might have reduced the thiol/epoxy interactions. The possible degradation of the SH-SAN-33 can be corroborated by looking at the TGA data which showed a 3% lost of SH-SAN-33 at 180°C (the annealing temperature).

Table 2 Summary of blend microstructure for extruded blends and annealed blends

Sample	SAN/PE (wt.%)	Annealing Conditions	$\langle D \rangle_{vs}$ (μm)
SH-SAN-33/E-PE	20 / 80	None	1.3
SH-SAN-33/E-PE	20 / 80	20 min @180 °C	2.5
SH-SAN-33/PE	20 / 80	None	3.7
SH-SAN-33/PE	20 / 80	20 min @180 °C	3.9

Reorientation of SAN Domains

A channel die was used to modify the morphology of the SAN domains within the E-PE matrix (Figure 6). The goal was to stretch the SAN droplets into lamellar structures, which would provide better barrier properties due to higher tortuosity within the blend.[16] The unidirectional flow within the channel die was achieved by pressing the extruded SH-SAN-33/E-PE blend samples into a rectangular shape that would fit the dimensions of the die well (Figure 7). However, this also added an extra application of heat (temperature high enough to melt the polymer) and shear (viscous dissipation) to the molten blend. For this reason, ESEM micrographs were taken to quantify if any changes in SAN domain size occurred (Figure 19 a, b). Images were taken in two perpendicular planes of the rectangles (as outlined in Figure 2) to ensure the observation of spherical SAN domains, if they were present. The $\langle D \rangle_{vs}$ values for the SH-SAN-33/E-PE blend were 1.2 μm and 1.5 μm for the direction 1 and 2 respectively.

The initial dimensions of the rectangular polymer blend samples were: length of 2 mm, height 15 mm and width 6 mm. After the samples were compressed within the channel die the dimensions were: length of 60 mm, height of 0.5 mm, and the width remained constant at 6 mm: giving an extension ratio of 30. ESEM images of the reoriented samples were taken to confirm the effect of uni-dimensional flow on the SAN domain size (Figure 19). The SAN domain surfaces in the cross direction (view 1, Figure 7) remained circular (Figure 19 a, b) while the surfaces in the perpendicular direction (view 2, Figure 7) become elongated domains (Figure 19 c, d). The elongated domains can be explained by the coalescence and

stretching of the initial droplets due to the uni-dimensional flow produced by the compression force. As a result of the reorientation process, a lamellar morphology of the SH-SAN-33 phase in the E-PE matrix was obtained.

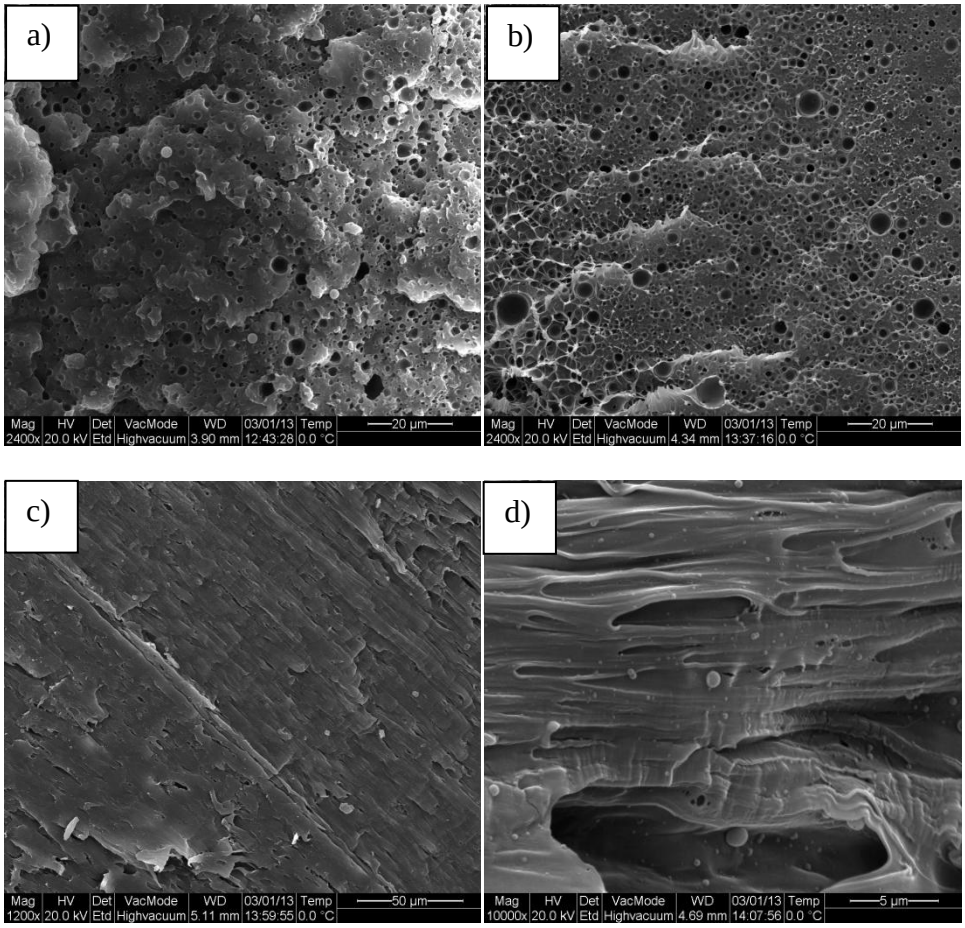

Figure 19 ESEM images of a) E-PE/SH-SAN-33 (80/20) pressed into rectangle (view 1), b) E-PE/SH-SAN-33 (80/20) pressed into rectangle (view 2), c) and d) E-PE/SH-SAN-33 (80/20) pressed in channel die (view 2)

2.4 Conclusions

The copolymerization of AN with ST to form statistical copolymers with thiol functionality at the chain end was performed in a controlled manner by RAFT and a subsequent chain end transformation by an aminolysis reaction. The copolymerization exhibited relatively narrow molecular weight distribution with

$\bar{M}_n$ = 31.4-37.6 kg·mol^{-1} and PDI = 1.3-1.4, and 35-40 mol.% AN. Functional SAN polymers were melt blended with epoxy functional PE and non-reactive PE. After melt blending in a twin-screw extruder at 180^{o}C, the resulting $\langle D \rangle_{vs}$ of the dispersed SAN phase was 1.3 μm for the functional blend and 3.7 μm for the non-functional blend. However, there was coarsening of the particles during the annealing process in the functional blend where the $\langle D \rangle_{vs}$ almost doubled. These results show that the thiol-epoxy interactions in the functional blend enabled compatibilization of the blend to an extent since the particle size in the functional blend was lower than the non-functional blend. The reactive blend exhibited a smaller particle size nevertheless even after annealing. In addition, the spherical SAN domains, obtained after extrusion, were stretched out to form a lamellar blend morphology in a channel die. These AN containing copolymers represent the first step towards the achievement of more complex microstructures that could be beneficial for the enhancement of barrier properties for materials intended for barrier applications.

3 Synthesis of ST/AN/GMA Random Copolymers by RAFT for Barrier Materials Useful for Blending Applications

3.1 Introduction

Melt blending of polyolefins such as PE with polyesters and polyamides as the dispersed phase is a useful method to improve the barrier properties against materials that can swell the PE.[16] The major problem with this approach is the lack of miscibility between the two phases to achieve the desirable morphology required for optimal barrier properties. As a result, compatibilization of the immiscible phases is required. Compatibilization can be achieved *in situ* by functionalizing the blend components in a process called reactive blending where the reactive groups present in the polymer components give rise to chemical reactions during melt blending process.[87] PE can be functionalized with functional groups such as carboxylic acid, epoxy or anhydride to form stable covalent bonds, given that the dispersed phase contains the corresponding complementary reactive group.[16, 17, 87] A dispersed phase can be suitably functionalized with the complementary functional group to react with the group on the polymer comprising the major phase, thereby producing the copolymer *in situ* at the interface between the two phases. For example, glycidyl methacrylate (GMA) was incorporated into PS, where the epoxy groups in GMA reacted with acid groups present in poly(ethylene terephthalate) to form the copolymer compatibilizer in the melt.[88]

AN containing copolymers such as SAN exhibited good barrier properties and improved processability compared to pure PAN homopolymer when ST was

copolymerized with AN.[16] SAN can be obtained by CRP techniques, which is an advantageous technique compared to conventional radical polymerization. CRP has the ability to make polymers with controlled microstructure which allows for block copolymers to be made. SAN has been synthesized using the most common CRP techniques: NMP,[24] ATRP,[25-27] and RAFT.[31, 33] SAN however lacks the functionality required for *in situ* compatibilization for blending applications. Here, SAN was made compatible by the addition of GMA to the polymerizing of AN and ST to make E-SAN. E-SAN possess multiple functional groups in the polymer chain which should increase the possibilities of copolymer formation during melt blending compared with the single functionality of SH-SAN used in Chapter 2. The epoxy groups present in E-SAN could be used to react with carboxylic acid groups that were grafted onto PE to form compatibilized blends. Specially, this chapter took the initial first steps by studying the random terpolymerization of GMA, ST and AN to form E-SAN, which can be used in melt blending applications with PE-COOH.

3.2 Experimental Section

Materials

ST (99%), AN (99%) and GMA (97%) were purchased from Sigma-Aldrich and purified to remove the inhibitor by passing through a column of basic alumina (Brockmann, Type 1, 150 mesh) mixed with 5% calcium hydride (90– 95%, reagent grade), then sealed with a head of nitrogen and stored in a refrigerator until needed. Methanol (99.8%), THF (99.9%), and DMF (99.8%) were obtained

from Fisher and used as received. DBTC (97%) was purchased from Strem Chemicals Inc and used as received. AIBN (90-95%) was purchased from Sigma-Aldrich and purified by recrystallization from methanol. $CDCl_3$ (>99%) was purchased from Cambridge Isotopes Laboratory and used as received as solvent for ^{13}C-NMR. Monocarboxy terminated PS (PS-COOH, $\bar{M}_w$ = 13 kg mol^{-1}, PDI = 1.01) was purchased from Scientific Polymer Products, inc.

Synthesis of ST/AN/GMA Terpolymers

The S/AN/GMA terpolymerization reactions by RAFT were conducted in 50 wt.% DMF solution at 80°C using DBTC as CTA and AIBN as initiator. The polymerizations were performed in a three-necked 25 mL round bottom flask equipped with a magnetic stirrer and a heating mantle/controller. A condenser connected to an ethylene glycol/water mixture recirculating chiller was attached to one neck of the flask to prevent the evaporation of the mixture components. The condenser was capped by a rubber septum with a needle to serve as an outlet for the nitrogen purge used. A thermal well attached to the temperature controller was connected to another port. The third port of the reactor was sealed with a rubber septum and was connected via a needle to a tank of nitrogen that supplied the purge to remove de-oxygenate. Detailed experimental conditions regarding the feed compositions are listed in Table 3. Note that the monomer to DBTC to AIBN concentration ratio was kept constant at 800:1:0.5. A formulation with an ST, AN and GMA initial feed molar compositions (f_{ST}, f_{AN} and f_{GMA} respectively) of 55%, 40% and 5% respectively, is given below as an example.

AIBN (0.015 g) and DBTC (0.051 g) were first added to the reactor followed by DMF (12.06 g) and previously purified ST (8.00 g), GMA (1.01 g) and AN (2.97 g). The reactor was sealed and then purged with nitrogen for 30 min. The reactor temperature was increased to 80°C at a rate of about 8.5ºC min^{-1} while maintaining the purge. When the temperature reached 70°C, the initial polymerization time was taken as this point. Samples were periodically removed and precipitated in methanol to allow kinetic data to be obtained by gravimetry. Typical polymerization times were about 360 min. The reaction mixture was allowed to cool to room temperature and then the final polymer was precipitated in methanol. The final polymer and the samples were vacuum filtered, and then dried overnight in a vacuum oven at 50°C to thoroughly remove any solvent and unreacted monomer. The target $\bar{M}_n$, calculated by the mass of monomers relative to the moles of DBTC, was set to 68 kg·mol^{-1} to ensure good entanglement between the polymer chains which translate into improve mechanical, rheological and adhesive properties of the blend.[4, 89] The final yield for the example given was 51% (6.1 g) after 378 min of polymerization with 36 kg·mol^{-1} $\bar{M}_n$ and PDI = 1.48 as determined by GPC calibrated relative to PS standards at 35°C in THF. The ST, AN and GMA molar composition of the copolymer (F_{ST}, F_{AN} and F_{GMA} respectively) as determined by ^{13}C NMR in $CDCl_3$ was 55%, 40% and 5%. The quaternary carbon resonance values of ST (146‑139 ppm), the nitrile carbon resonance values of AN (122‑117 ppm) and the quaternary carbon resonance values of GMA (172‑178 ppm) were used to determine the molar composition of the polymers.

The theoretical $\bar{M}_n$ ($\bar{M}_{n,th}$) was calculated using the following equation:

$$\bar{M}_{n,th} = \frac{[ST] \cdot M_{ST} \cdot f_{\mathrm{ST}} + [AN] \cdot M_{AN} \cdot f_{\mathrm{AN}} + [GMA] \cdot M_{GMA} \cdot f_{\mathrm{GMA}}}{[DBTC]} \cdot x + M_{DBTC}$$

where, [ST], [AN], [GMA], and [DBTC] are the initial concentrations of ST, AN, GMA and DBTC, and M_{ST}, M_{AN}, M_{GMA} and M_{DBTC} are the molecular weights of ST, AN, GMA and DBTC, respectively. This equation assumes an ideal RAFT system where the polymers directly derived from the initiator are thought to be minimal.[32]

Table 3 Experimental Conditions for S/AN/GMA Terpolymerizations at 80°C in DMF DBTC and AIBN

Experiment ID[a]	$[DBTC]_0$ (mol/L)	$[AIBN]_0$ (mol/L)	$[ST]_0$ (mol/L)	$[AN]_0$ (mol/L)	$[GMA]_0$ (mol/L)	$[DMF]_0$ (mol/L)
AN-GMA-ST-40-05	6.8×10^{-3}	3.5×10^{-3}	2.9	2.2	0.3	6.4
AN-GMA-ST-40-10	6.5×10^{-3}	3.3×10^{-3}	2.6	2.1	0.5	6.5
AN-GMA-ST-40-20	6.5×10^{-3}	3.2×10^{-3}	2.0	2.0	1.0	6.5

[a]Experimental ID is given by the following notation AN-GMA-ST-xx-yy where xx and yy represent the f_{AN} and f_{GMA} respectively.

Melt Blending of ST/AN/GMA Terpolymers and PS-COOH

AN-GMA-ST-40-5 (0.46 g) and PS-COOH (0.50 g) were mechanically mixed at room temperature, and then fed into a miniature twin screw extruder at 180°C operated at a screw speed of 150 rpm. The blending process lasted 5 minutes, after which the blend was scraped off the screws since there was not enough material to exit through the die. The polymers were characterized using GPC against PS standards at 35°C in THF.

Characterization

$\bar{M}_n$, $\bar{M}_w$ and PDI were estimated using GPC (Waters Breeze) with DMF as the mobile phase at a flow rate of 0.3 mL·min^{-1}. The GPC was equipped with three Styragel® HR columns (HR1 with $\bar{M}_n$ measurement range of 0.1 to 0.5 kg·mol^{-1}, HR2 with $\bar{M}_n$ measurement range of 0.5 to 20 kg·mol^{-1} and HR4 with $\bar{M}_n$ measurement range of 5 to 600 kg·mol^{-1}) and a guard column. The columns were kept at 35 °C during the analysis and the molecular weights were estimated relative to linear PS standards. The GPC was equipped with both differential RI (2410) and UV (2487) detectors for which the RI detector was used solely for the experiments described herein. ^{13}C NMR was performed with a 500 MHz Varian Mercury instrument with a total of 1024 scans on each sample to determine the molar compositions of E-SAN copolymers. The quaternary carbon resonance values of ST (146–139 ppm), the nitrile carbon resonance values of AN (122–117 ppm) and the quaternary carbon resonance values of GMA (172–178 ppm) were used for the determination of the ST, GMA and AN polymer content (Figure 20).[90]

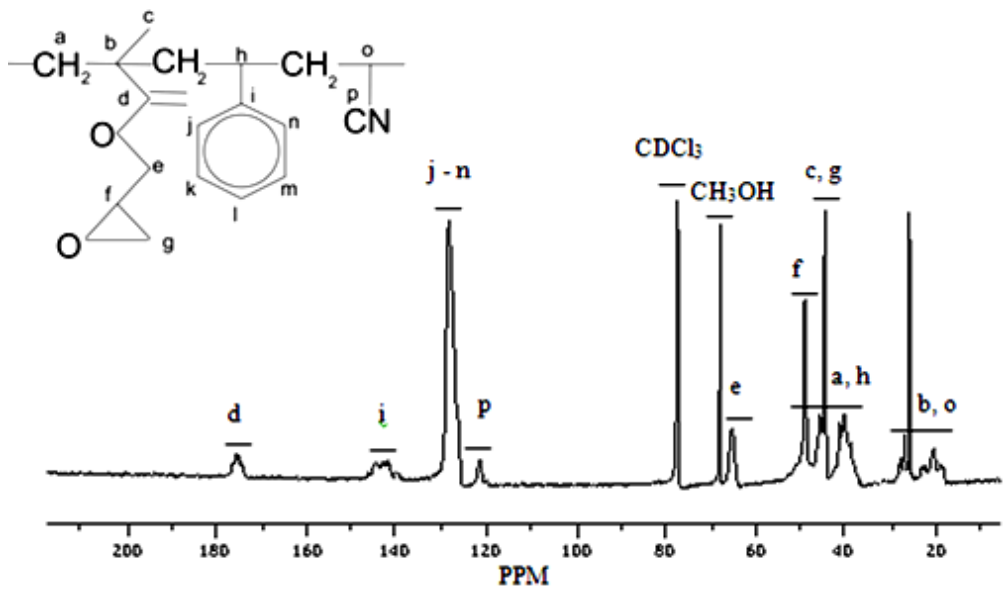

Figure 20: ^{13}C NMR spectrum of ST/AN/GMA terpolymers prepared by RAFT with DBTC and AIBN in 50 wt.% DMF solution at 80°C using $CDCl_3$ as solvent ([monomers]/[DBTC]/[AIBN] = 800:1:0.5, [ST]/[AN]/[GMA] = 40:40:20, x = 56%).

3.3 Results and Discussion

Synthesis of ST/AN/GMA Terpolymers

The RAFT terpolymerization of ST, GMA and AN was performed using DBTC as CTA and AIBN as initiator. This particular terpolymerization has not been done via RAFT previously. However, RAFT with DBTC as CTA has been used to synthesize PS and PAN homopolymers.[32, 79] Semilogarithmic kinetic plots of monomer conversion versus time for the three different initial molar feed compositions investigated are indicated in Figure 21. The semilogarithmic plots exhibited linear behaviour for the first 200 min of polymerization. The apparent rate constants were calculated from the slopes of the semilogarithmic plots by using five to six sample points from the linear region. The apparent rate constants

were found to be 0.003 min^{-1}, 0.005 min^{-1}, 0.005 min^{-1} for ST-AN-GMA-55-40-05, ST-AN-GMA-50-40-10, ST-AN-GMA-40-40-20; the apparent rate constant increased slightly with increasing f_{GMA}. The apparent rate constant for the copolymerization with 5% f_{GMA} was similar to previous polymerizations of SAN (see Chapter 2 of this thesis) and Fan et al work.[31] Figure 22 exhibits the $\bar{M}_n$ and PDI versus conversions for the three molar feed compositions investigated. The polymerizations exhibited linear evolution of $\bar{M}_n$ with conversion together with linear evolution of the semilogarithmic plots up to 200 min. The semilogarithmic plots of ST-AN-GMA-50-40-10 and ST-AN-GMA-40-40-20 exhibited some non-linearity after 200 min where conversion reached a constant value. Preparation of polymers with PDI of < 1.50 and $\bar{M}_n$ ranging from 34.4-38.3 $kg \cdot mol^{-1}$ was observed. PDIs decreased with increasing conversion and the final values range from 1.38-1.48 which are consistent with GMA polymerizations by RAFT and slightly lower or similar to the PDI values obtained by the ST/AN/GMA normal free radical terpolymerization (PDIs > 1.43).[91, 92] The composition of E-SAN was found using ^{13}C NMR and the results are reported in Table 4. The polymerizations at higher f_{GMA} showed a compositional drift towards both ST and GMA which is consistent literature. [93]

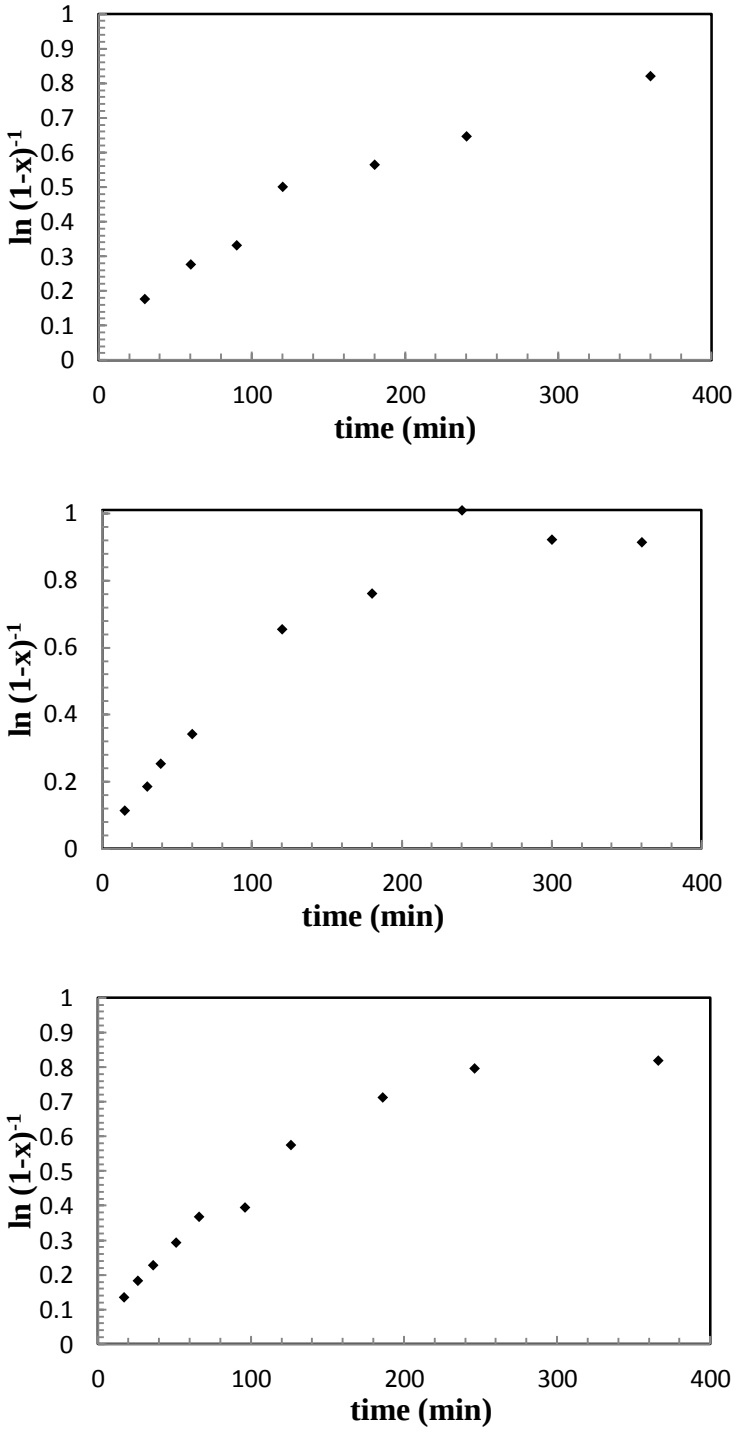

Figure 21: Scaled conversion (ln $(1-x)^{-1}$) for the ST-AN-GMA random terpolymerizations done in 50 wt.% DMF at 80°C in the presence of DBTC and AIBN at the following initial % molar feed fraction: (a) f_{ST} = 55, f_{AN} = 40, f_{GMA} = 5, (b) f_{ST} = 50, f_{AN} = 40, f_{GMA} = 10 and (c) f_{ST} = 40, f_{AN} = 40, f_{GMA} = 20.

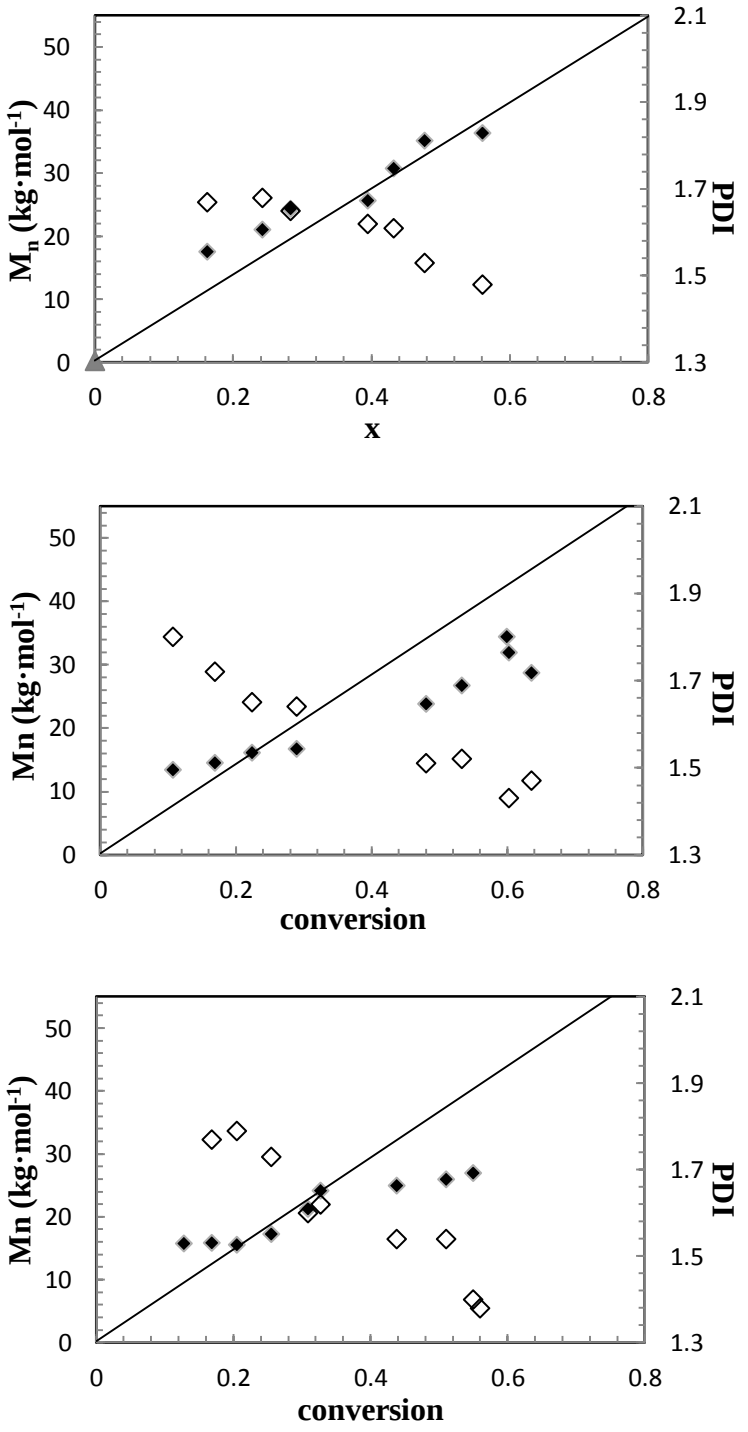

Figure 22: $\bar{M}_n$ and PDI measured by GPC relative to PS standards versus conversion for ST-AN-GMA random terpolymers synthesized with 50 wt.% monomer solution in DMF at 80°C in the presence of DBTC and AIBN at the following initial % molar feed fraction: (a) f_{ST} = 55, f_{AN} = 40, f_{GMA} = 5, (b) f_{ST} = 0.50, f_{AN} = 40, f_{GMA} = 10 and (c) f_{ST} = 40, f_{AN} = 40, f_{GMA} = 20. The straight lines indicate the theoretical $\bar{M}_n$ vs. conversion. $\bar{M}_n$ is indicated by filled squares (■) and PDI is indicated by open squares (□).

Table 4 Characterization of ST/AN/GMA Random Terpolymers Synthesized at 80°C in 50 wt.% DMF Solution using DBTC and AIBN

experiment ID	$f_{AN,0}$	$f_{GMA,0}$	F_{AN}[a]	F_{GMA}[a]	conversion (%)	$\bar{M}_n$ (kg mol^{-1})[b]	PDI[b]
AN-GMA-ST-40-05	40	5	40	6	56	34.8	1.48
AN-GMA-ST-40-10	40	10	36	11	60	34.4	1.45
AN-GMA-ST-40-20	40	20	29	26	56	38.3	1.38

[a] F_{AN} and F_{GMA} were determined using ^{13}C-NMR. [b] $\bar{M}_n$ and PDI determined by GPC relative to PS standards in THF at 35°C.

Melt Blending of ST/AN/GMA Terpolymers and PS-COOH

E-SAN was melt-blended with PS-COOH to evaluate the reactivity of the epoxy/acid reaction using GPC. This was done to estimate the effect of reaction for the blend of interest, PE-COOH/E-SAN since there is no common solvent available for PE and SAN. Copolymer formation for the PE-COOH/E-SAN system cannot be directly measured by GPC since there is not a common solvent between them. The polymers were mechanically blended by hand in a beaker at room temperature, and then fed into a miniature twin-screw extruder at 180°C operated at a screw speed of 150 rpm. The reactivity of the epoxy-carboxylic acid reaction in the present conditions was addressed by GPC and the results are presented in Figure 23. The peak of the blend showed little difference from the peaks of the individual polymers which indicated the absence of the epoxy-carboxylic acid reaction during the blending process. The epoxy-carboxylic acid reaction has been used successfully for the reactive blending of carboxy-functional nitrile rubber powder and polypropylene functionalized with GMA at a

higher temperature (200°C); the *in situ* compatibilization was confirmed by FT-IR.[94] The blending was performed in a twin-screw extruder in the absence of a catalyst. Taha et al. reported that the conversion of epoxy groups in batch reactors at 180°C after 10 min is low (lower than 30% calculated by FT-IR).[95] Taha's work consisted in the reaction of a miscible solution of low molar mass epoxy prepolymers, bisphenol A and carboxy terminated butadiene-AN random copolymer based rubber inside a twin-screw extruder. Taha et al. decided to use a catalyst since the residence time of reactants within the extruder was between 1 and 5 min, similar to the current study. Taha's group used triphenyl phosphine as catalyst and conversions higher than 80 % calculated by FT-IR were obtained at 180°C in a twin extruder.[95] The use of a catalyst during the blending process could accelerate the reaction between the epoxy groups in E-SAN and the carboxylic acid groups in PE-COOH. The use of a catalyst during blending would help to observe if the results obtained by Taha's group using small molecules could be achieved in polymeric reactions.

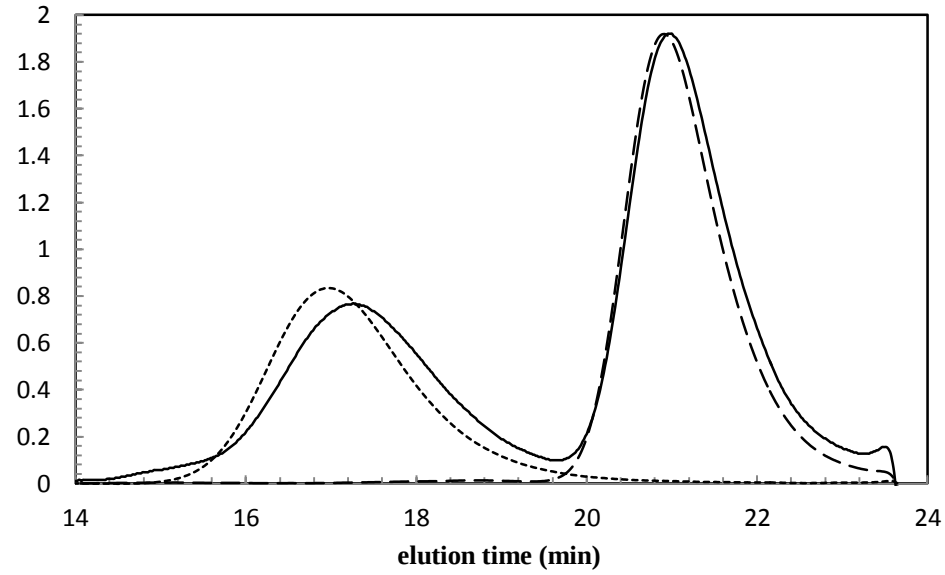

Figure 23: GPC of E-SAN (dotted line), PS-COOH (dashed line), and the blend between E-SAN and PS-COOH performed in miniature twin screw extruder at 180°C and a screw speed of 150 rpm (solid line).

3.4 Conclusions

E-SAN was synthesized by the terpolymerization of ST/AN/GMA by RAFT in DMF solution using DBTC as CTA and AIBN as initiator at 80ºC. E-SAN copolymers at varying f_{GMA} exhibited relatively narrow molecular weight distribution (PDI < 1.5); $\bar{M}_n$ up to 38.3 kg·mol^{-1}, and 29-40 mol.% AN content. The composition of GMA in the terpolymers was greater than in the feed and apparently increased as the f_{GMA} increased. The blending of E-SAN with PS-COOH in a twin-screw extruder revealed that the epoxy-carboxylic acid reaction between the functional groups present in E-SAN and PS-COOH do not take place in the absence of a catalyst and at the extrusion conditions used in this study (180ºC, 5 min residence time, 150 rpm).

4 Considerations for Future Work

The reaction between a thiol and an epoxy group has not been used in melt blending processes despite its success in industrial and biomedical applications likely because it requires a catalyst.[10] Sunggak et al. work on small molecules involving thiols and alcohols reactions with carboxylic acids reported high yields when using 4-dimethylamino-pyridine as a catalyst.[96] The incorporation of a catalyst to the *in situ* compatibilization of the SAN/PE blend could improve the morphology of the system by enhancing the thiol/epoxy reaction.

The epoxy-carboxylic acid coupling has been effective during melt blending processes at temperatures between 260°C and 270°C but without conclusive proof of reaction.[88] Consequently, increasing the temperature of the extrusion process to temperatures > 250°C could allow the thiol-epoxy and the epoxy-carboxylic acid reactions to take place. The drawback with increasing the extrusion temperature is the possible degradation of the polymers during the blending process. In another work, Taha et al. reported that the conversion of epoxy groups in batch reactors at 180°C after 10 min is less than 30% and concluded that a catalyst was needed to achieve higher conversions (> 80%) especially considering that the residence time within a extruder is between 1 and 5 min.[95] Triphenyl phosphine was used by Taha's group as a catalyst for the epoxy/carboxylic acid reaction present in the formation of high molar mass epoxy prepolymers containing rubber dispersions based on carboxyl-terminated butadiene–AN random copolymer.[95] The conversion obtained by Taha et al. was higher than 80% and conclusive evidence of the reaction was obtained by FT-IR.[95] Polyesters containing a metal catalyst have been used for the reactive

compatibilization of polyesters and epoxy containing polymers by Stewart et al.[97] The melt blending of the polyester and the epoxy containing copolymer was performed in batch using a rheometer at 50 rmp and a set point temperature of 270ºC using 60 g samples. Stewart's group concluded that polyesters containing antimony are particularly effective at promoting the reaction between polyesters and either ethylene-co-GMA or ST-co-GMA copolymers.

An alternative to the epoxy/carboxylic acid reaction for *in situ* compatibilization of blends in extrusion process could be the thiol/anhydride reaction. The thiol/anhydride reaction in small molecules can be catalyzed by cobalt(II) chloride with excellent yields results.[98] Thiols have also been reacted with cyclic anhydrides in the presence of a basic catalyst under anhydrous conditions with high yields as well.[99] Thiol terminated poly(*N*,*N*-diethylacrylamide) was used as a macroinitator for ring opening polymerization of γ-benzyl-L-glutamate *N*-carboxyanhydrade.[100] To the knowledge of the author the thiol/anhydride reaction has not been used in blends in extrusion processes. The effectiveness of the SH-SAN/E-PE blend as barrier material for fuel tanks applications needs to be tested as well.

5 General Conclusion

This study showed the preparation of AN containing copolymer by RAFT, as a first step towards using AN-based polymers for barrier materials in polyolefins. Eventually, using RAFT permits the possibility of using microstructured copolymers to impart more sophisticated morphologies and properties into barrier materials. The copolymerization was followed by an aminolysis reaction that took

advantage of the CTA retained after polymerization and provided thiol functionality to the polymer which was used in a reactive blending application. The thiol-epoxy reaction was studied by blending of SH-SAN with E-PS in a twin-screw extruder and based on the GPC analysis; the thiol-epoxy reaction did not take place. The functional SH-SAN copolymer was melt blended with E-PE and non-functional PE in a miniature twin screw extruder. The resulting particle size of the dispersed SAN phase was finer in the SH-SAN/E-PE (1.3 μm) blend compared to the SH-SAN/PE (3.7 μm) blend, suggesting that the thiol-epoxy interaction between the polymers enables compatibilization of the blend. However, there was coarsening of the particles during the annealing process in the SH-SAN/E-PE where the particle size increased to 2.5 μm. The coarsening of the particles after blending is an indication that the thiol/epoxy interactions were not completely stable. In addition, the spherical SAN domains, obtained after extrusion, were stretched out to form a lamellar blend structure in a channel die.

The second part of the study showed the preparation of ST/AN/GMA terpolymers by RAFT at varying GMA feed concentrations, f_{GMA}. E-SAN copolymers at varying f_{GMA} exhibited relatively narrow molecular weight distribution (PDI < 1.5); $\bar{M}_n$ up to 38.3 kg·mol^{-1}, and 29-40 mol.% AN content. The composition of GMA in the terpolymers was greater than in the feed and apparently increased with increasing f_{GMA}. Similar to the thiol-epoxy reaction, the epoxy-carboxylic acid reaction which was studied by blending of E-SAN with PS-COOH in a twin-screw extruder did not take place under the conditions here described and as suggested by Taha et al. might require the use of a catalyst.[95]

6 References

[1] Koning, C.; Van Duin, M.; Pagnoulle, C.; Jerome, R., *Progress in Polymer Science*, (1998) **23**, 707.

[2] Robert J. Young, P. A. L., *Introduction to Polymers*, Taylor & Francis Group, LLC: Boca Raton, FL, United States, (2011).

[3] Z. Horak, I. F., J. Kolarik, D.Hlavata, A. Sikora, Polymer Blends, In *Encyclopedia of Polymers Science and Technology*, John Wiley & Sons, Inc: (2002).

[4] Ashcraft, E.; Ji, H.; Mays, J.; Dadmun, M., *ACS Applied Materials & Interfaces*, (2009) **1**, 2163.

[5] Guegan, P.; Macosko, C. W.; Ishizone, T.; Hirao, A.; Nakahama, S., *Macromolecules*, (1994) **27**, 4993.

[6] Orr, C. A.; Adedeji, A.; Hirao, A.; Bates, F. S.; Macosko, C. W., *Macromolecules*, (1997) **30**, 1243.

[7] Jeon, H. K.; Zhang, J.; Macosko, C. W., *Polymer*, (2005) **46**, 12422.

[8] Moon, B.; Hoye, T. R.; Macosko, C. W., *Macromolecules*, (2001) **34**, 7941.

[9] Karavia, V.; Deimede, V.; Kallitsis, J. K., *Journal of Macromolecular Science, Part A*, (2004) **41**, 115.

[10] De, S.; Khan, A., *Chemical Communications*, (2012) **48**, 3130.

[11] Roth, P. J.; Boyer, C.; Lowe, A. B.; Davis, T. P., *Macromolecular Rapid Communications*, (2011) **32**, 1123.

[12] Yamamoto, T.; Ishidoya, M., *Progress in Organic Coatings*, (2000) **40**, 267.

[13] Rodriguez, F.; Cohen, C.; Ober, C., K,; Archer, L. A., *Principles of Polymer Systems. 5th ed.*, Taylor & Francis: New York, NY, (2003).

[14] Yeh, J.-T.; Huang, S.-S.; Yao, W.-H., *Macromolecular Materials and Engineering*, (2002) **287**, 532.

[15] DeLassus, P., *Barrier Polymers in Kirk-Othmer Encyclopedia of Chemical Technology*, (2002); pp 375.

[16] Subramanian, P. M.; Mehra, V., *Polymer Engineering & Science*, (1987) **27**, 663.

[17] Pracella, M.; Chionna, D.; Pawlak, A.; Galeski, A., *Journal of Applied Polymer Science*, (2005) **98**, 2201.

[18] Subramanian, P. M., *Polymer Engineering & Science*, (1985) **25**, 483.

[19] Szwarc, M., *Nature*, (1956) **178**, 1168.

[20] Conlon, D. A.; Crivello, J. V.; Lee, J. L.; O'Brien, M. J., *Macromolecules*, (1989) **22**, 509.

[21] Fetters, L. J.; Morton, M., *Macromolecules*, (1969) **2**, 453.

[22] Moad, G.; Rizzardo, E.; Thang, S. H., *Australian Journal of Chemistry*, (2009) **62**, 1402.

[23] Graeme Moad, D. H. S., *The Chemistry of Radical Polymerization Second fully revised edition*, Elsevier iNC,: San Diego. C A, (2006).

[24] Nicolas, J.; Brusseau, S.; Charleux, B., *Journal of Polymer Science Part A: Polymer Chemistry*, (2010) **48**, 34.

[25] Al-Harthi, M.; Sardashti, A.; Soares, J. B. P.; Simon, L. C., *Polymer*, (2007) **48**, 1954.
[26] Tsarevsky, N. V.; Sarbu, T.; Göbelt, B.; Matyjaszewski, K., *Macromolecules*, (2002) **35**, 6142.
[27] Pietrasik, J.; Dong, H.; Matyjaszewski, K., *Macromolecules*, (2006) **39**, 6384.
[28] Tang, C.; Kowalewski, T.; Matyjaszewski, K., *Macromolecules*, (2003) **36**, 8587.
[29] Liu, X.-H.; Zhang, G.-B.; Lu, X.-F.; Liu, J.-Y.; Pan, D.; Li, Y.-S., *Journal of Polymer Science Part A: Polymer Chemistry*, (2006) **44**, 490.
[30] An, Q.; Qian, J.; Yu, L.; Luo, Y.; Liu, X., *Journal of Polymer Science Part A: Polymer Chemistry*, (2005) **43**, 1973.
[31] Fan, D.; He, J.; Xu, J.; Tang, W.; Liu, Y.; Yang, Y., *Journal of Polymer Science Part A: Polymer Chemistry*, (2006) **44**, 2260.
[32] Liu, X.-H.; Li, Y.-G.; Lin, Y.; Li, Y.-S., *Journal of Polymer Science Part A: Polymer Chemistry*, (2007) **45**, 1272.
[33] Božović-Vukić, J.; Mañon, H. T.; Meuldijk, J.; Koning, C.; Klumperman, B., *Macromolecules*, (2007) **40**, 7132.
[34] Debuigne, A.; Michaux, C.; Jérôme, C.; Jérôme, R.; Poli, R.; Detrembleur, C., *Chemistry – A European Journal*, (2008) **14**, 7623.
[35] Tonnar, J.; Lacroix-Desmazes, P.; Boutevin, B., *Macromolecules*, (2006) **40**, 186.
[36] Wu, M. M., Acrylonitrile and Acrylonitrile Polymers, In *Encyclopedia of Polymer Science and Technology*, John Wiley & Sons, Inc.: (2002).
[37] Wang, J.-S.; Matyjaszewski, K., *Macromolecules*, (1995) **28**, 7901.
[38] Patten, T. E.; Matyjaszewski, K., *Advanced Materials*, (1998) **10**, 901.
[39] Tasdelen, M. A.; Kahveci, M. U.; Yagci, Y., *Progress in Polymer Science*, (2011) **36**, 455.
[40] Matyjaszewski, K.; Xia, J., *Chemical Reviews*, (2001) **101**, 2921.
[41] Jakubowski, W.; Kirci-Denizli, B.; Gil, R. R.; Matyjaszewski, K., *Macromolecular Chemistry and Physics*, (2008) **209**, 32.
[42] Solomon, D. H., *Journal of Polymer Science Part A: Polymer Chemistry*, (2005) **43**, 5748.
[43] Georges, M. K.; Veregin, R. P. N.; Kazmaier, P. M.; Hamer, G. K., *Macromolecules*, (1993) **26**, 2987.
[44] Gabaston, L. I.; Jackson, R. A.; Armes, S. P., *Macromolecules*, (1998) **31**, 2883.
[45] Tang, C.; Kowalewski, T.; Matyjaszewski, K., *Macromolecules*, (2003) **36**, 1465.
[46] Sciannamea, V.; Jerome, R.; Detrembleur, C., *Chemical Reviews*, (2008) **108**, 1104.
[47] Zetterlund, P. B., *Macromolecular Reaction Engineering*, (2010) **4**, 663.
[48] Couvreur, L.; Lefay, C.; Belleney, J.; Charleux, B.; Guerret, O.; Magnet, S., *Macromolecules*, (2003) **36**, 8260.
[49] Benoit, D.; Harth, E.; Fox, P.; Waymouth, R. M.; Hawker, C. J., *Macromolecules*, (2000) **33**, 363.

[50] Schierholz, K.; Givehchi, M.; Fabre, P.; Nallet, F.; Papon, E.; Guerret, O.; Gnanou, Y., *Macromolecules*, (2003) **36**, 5995.
[51] Charleux, B.; Nicolas, J.; Guerret, O., *Macromolecules*, (2005) **38**, 5485.
[52] Nicolas, J.; Dire, C.; Mueller, L.; Belleney, J.; Charleux, B.; Marque, S. R. A.; Bertin, D.; Magnet, S.; Couvreur, L., *Macromolecules*, (2006) **39**, 8274.
[53] Ilhanli, O. B.; Erdogan, T.; Tunca, U.; Hizal, G., *Journal of Polymer Science Part A: Polymer Chemistry*, (2006) **44**, 3374.
[54] Consolante, V.; Maric, M.; Penlidis, A., *Journal of Applied Polymer Science*, (2012) **125**, 3963.
[55] Rizzardo, E.; Moad, G.; Thang, S. H., RAFT Polymerization in Bulk Monomer or in (Organic) Solution, In *Handbook of RAFT Polymerization*, Wiley-VCH Verlag GmbH & Co. KGaA: (2008); pp 189.
[56] Krstina, J.; Moad, G.; Rizzardo, E.; Winzor, C. L.; Berge, C. T.; Fryd, M., *Macromolecules*, (1995) **28**, 5381.
[57] Chiefari, J.; Chong, Y. K.; Ercole, F.; Krstina, J.; Jeffery, J.; Le, T. P. T.; Mayadunne, R. T. A.; Meijs, G. F.; Moad, C. L.; Moad, G.; Rizzardo, E.; Thang, S. H., *Macromolecules*, (1998) **31**, 5559.
[58] Keddie, D. J.; Guerrero-Sanchez, C.; Moad, G.; Mulder, R. J.; Rizzardo, E.; Thang, S. H., *Macromolecules*, (2012) **45**, 4205.
[59] Willcock, H.; O'Reilly, R. K., *Polymer Chemistry*, (2010) **1**, 149.
[60] Moad, G.; Rizzardo, E.; Thang, S. H., *Australian Journal of Chemistry*, (2006) **59**, 669.
[61] Moad, G.; Rizzardo, E.; Thang, S. H., *Polymer*, (2008) **49**, 1079.
[62] Moad, G.; Rizzardo, E.; Thang, S. H., *Australian Journal of Chemistry*, (2005) **58**, 379.
[63] Rodriguez-Veloz, O.; Kamal, M. R., *Advances in Polymer Technology*, (1999) **18**, 89.
[64] Padwa, A. R., *Polymer Engineering & Science*, (1992) **32**, 1703.
[65] Gromadzki, D.; Lokaj, J.; Černoch, P.; Diat, O.; Nallet, F.; Štěpánek, P., *European Polymer Journal*, (2008) **44**, 189.
[66] Qiu, X.-P.; Winnik, F. M., *Macromolecular Rapid Communications*, (2006) **27**, 1648.
[67] Roth, P. J.; Kessler, D.; Zentel, R.; Theato, P., *Journal of Polymer Science Part A: Polymer Chemistry*, (2009) **47**, 3118.
[68] Li, M.; De, P.; Gondi, S. R.; Sumerlin, B. S., *Journal of Polymer Science Part A: Polymer Chemistry*, (2008) **46**, 5093.
[69] Moad, G.; Chen, M.; Haussler, M.; Postma, A.; Rizzardo, E.; Thang, S. H., *Polymer Chemistry*, (2011) **2**, 492.
[70] Derek L. Patton, M. M.; Timothy Fulghum, a. R. C. A., *Macromolecular Materials and Engineering*, (2005) **38**, 8597.
[71] Lowe, A. B., *Polymer Chemistry*, (2010) **1**, 17.
[72] Yamashita, K.; Saba, H.; Tsuda, K., *Journal of Macromolecular Science: Part A - Chemistry*, (1989) **26**, 1291.
[73] Watanabe, S.; Ikeda, R.; Ikeda, H.; Murata, M.; Masuda, Y., *Polymer Journal*, (2004) **36**, 45.
[74] Drzal, P. L.; Barnes, J. D.; Kofinas, P., *Polymer*, (2001) **42**, 5633.

[75] Oxby, K. J.; Marić, M., *Macromolecular Reaction Engineering*, (2013), n/a.
[76] Marić, M.; Macosko, C. W., *Polymer Engineering & Science*, (2001) **41**, 118.
[77] Maric, M.; Consolante, V., *Journal of Applied Polymer Science*, (2013) **127**, 3645.
[78] Sanghvi, P. G.; Patel, A. C.; Gopalkrishnan, K. S.; Devi, S., *European Polymer Journal*, (2000) **36**, 2275.
[79] Feng, L.; Cavicchi, K. A.; Katzenmeyer, B. C.; Wesdemiotis, C., *Journal of Polymer Science Part A: Polymer Chemistry*, (2011) **49**, 5100.
[80] Boyer, C.; Granville, A.; Davis, T. P.; Bulmus, V., *Journal of Polymer Science Part A: Polymer Chemistry*, (2009) **47**, 3773.
[81] Cheremisinoff, N. P., *Advanced Polymer Processing Operations* Noyes Publications: United States of America, (1998).
[82] Wu, S., *Polymer Engineering & Science*, (1987) **27**, 335.
[83] Grace†, H. P., *Chemical Engineering Communications*, (1982) **14**, 225.
[84] Favis, B. D.; Chalifoux, J. P., *Polymer Engineering & Science*, (1987) **27**, 1591.
[85] Sundararaj, U.; Macosko, C. W., *Macromolecules*, (1995) **28**, 2647.
[86] Wildes, G.; Keskkula, H.; Paul, D. R., *Journal of Polymer Science Part B: Polymer Physics*, (1999) **37**, 71.
[87] Saleem, M.; Baker, W. E., *Journal of Applied Polymer Science*, (1990) **39**, 655.
[88] Maa, C.-T.; Chang, F.-C., *Journal of Applied Polymer Science*, (1993) **49**, 913.
[89] Wu, S., *Polymer*, (1987) **28**, 1144.
[90] Barron, P. F.; Hill, D. J. T.; O'Donnell, J. H.; O'Sullivan, P. W., *Macromolecules*, (1984) **17**, 1967.
[91] Zhu, J.; Zhou, D.; Zhu, X.; Chen, G., *Journal of Polymer Science Part A: Polymer Chemistry*, (2004) **42**, 2558.
[92] Gunaydin, O.; Yilmaz, F., *Polym. J*, (2007) **39**, 579.
[93] Brar, A. S.; Pradhan, D. R., *Journal of Applied Polymer Science*, (2003) **89**, 1779.
[94] Xu, X.; Qiao, J.; Yin, J.; Gao, Y.; Zhang, X.; Ding, Y.; Liu, Y.; Xin, Z.; Gao, J.; Huang, F.; Song, Z., *Journal of Polymer Science Part B: Polymer Physics*, (2004) **42**, 1042.
[95] Taha, M.; Perrut, V.; Roche, A. A.; Pascault, J. P., *Journal of Applied Polymer Science*, (1997) **65**, 2447.
[96] Sunggak, K.; Jae, I. L.; Young, K. K., *Tetrahedron Letters*, (1984) **25**, 4943.
[97] Stewart, M. E.; George, S. E.; Miller, R. L.; Paul, D. R., *Polymer Engineering & Science*, (1993) **33**, 675.
[98] Ahmad, S.; Iqbal, J., *Tetrahedron Letters*, (1986) **27**, 3791.
[99] Zienty, F. B.; Vineyard, B. D.; Schleppnik, A. A., *The Journal of Organic Chemistry*, (1962) **27**, 3140.
[100] Zhang, X.; Oddon, M.; Giani, O.; Monge, S.; Robin, J.-J., *Macromolecules*, (2010) **43**, 2654.